Annals of Mathematical Sciences and Applications
Volume 1, Number 2, 427–471, 2016

Mathematical models of morphogen dynamics and growth control

Jinzhi Lei*, Wing-Cheong Lo* and Qing Nie†

Morphogens are diffusive molecules produced by cells, sending signals to neighboring cells in tissues for communication. As a result, tissues develop cellular patterns that depend on the concentration levels of the morphogens. The formation of morphogen gradients is among the most fundamental biological processes during development, regeneration, and disease. During the past two decades, sophisticated mathematical models have been utilized to decipher the complex biological mechanisms that regulate the spatial and temporal dynamics of morphogens. Here, we review the model formulations for morphogen systems and present the mathematical questions and challenges that arise from the model analysis, with an emphasis on Drosophila. We discuss several important aspects of modeling frameworks: robustness, stochastic dynamics, growth control, and mechanics of morphogen-mediated patterning.

AMS 2000 subject classifications: Primary 92C15, 35K57; secondary 34B08, 92B05.
Keywords and phrases: Pattern formation, morphogen gradients, robustness, boundary value problem, reaction-diffusion equations.

1. Introduction

How distinct cell types and organs are generated from a single cell or a small number of cells is a fundamental question in studying multicellular organisms. The concept of the morphogen is at the center of answering this question [17, 130]. Morphogens are signaling molecules that can diffuse and act over several cell diameters to induce concentration-dependent cellular responses. This process involves various control strategies due to the complexity and diversity among different types of organ development. 'Wet' experiments alone are usually insufficient for understanding the complex machineries used for morphogen-mediated patterning and growth control.

*Co-first author.
†Corresponding author.

In recent years, the mathematical modeling approach has played a critical role in delineating these complex processes, as well as the principles behind them, providing an influx of fresh ideas and novel methods to biology [47, 55, 59, 86].

This review focuses on mathematical models of morphogen gradient formation, patterning robustness, and growth control, with an emphasis on Drosophila. We begin the review with a brief description of the biological background for morphogen systems. Next, we address general mathematical formulations for several typical models of morphogen gradient systems. We then discuss the robustness of morphogen gradients. Finally, we consider morphogen-mediated growth control models that are closely related to the scaling solutions and moving boundary problems. In this review, we focus mainly on morphogen dynamics and growth driven by localized sources of morphogens. Spontaneous patterning and some other aspects of patterning studies can be found in other reviews [18, 80, 86, 121, 128].

2. Biological background

In 1969, Wolpert proposed that cells acquire positional information, such as in a coordinate system, to produce spatial patterns of cellular fates [133]. Recently, substantial experimental evidence has shown that the positional information of cells strongly depends on various types of signaling molecules known as *morphogens* (aka ligands). For example, during embryonic development, morphogens are sythesized at a localized site and dispersed (e.g., through diffusion) from their production site to bind to cell receptors on cell membranes. These processes result in different levels of receptor occupancy at different cell locations, leading to different levels of downstream signals for different cells. The spatial concentration gradient of morphogen-receptor complexes (aka *signaling gradients*) induces spatially graded differences in cell signaling. These signaling gradients provide positional information for the global patterns across the target tissue [133, 134]. An important concept to understand is how cells know precisely and reliably where they are [60].

Morphogen-mediated pattern formation can be illustrated by a simple non-biological system: the patterning of French flag (Fig. 1), which has a simple pattern of one-third blue, one-third white, and one-third red in one direction, similar to a line of cells with three different fates. In this system, each cell has the potential to become blue, white, or red. One of the simplest ways of achieving this patterning is that the cells acquire positional information through the spatial gradient of the morphogen. If there is a source of morphogen at one end and a sink at the other end, the morphogen diffuses

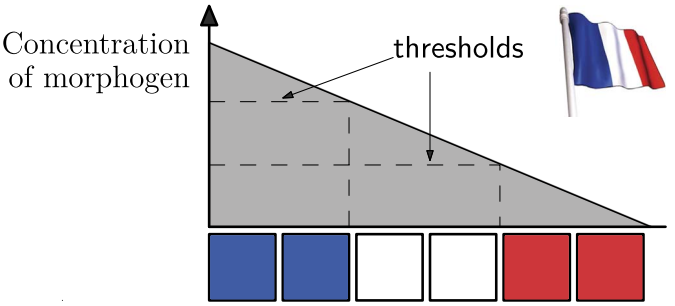

Figure 1: The French flag model of pattern formation (replotted from [135]).

along the line of cells, leading to graded concentrations in space, with different positional information for each spatial region. If the cells respond to *threshold concentrations* of the morphogen — for example, becoming blue, white, or red in accordance with high, middle, or low level morphogen concentrations — the line of cells then develops to become a French flag (Fig. 1).

Much of the experimental evidence for morphogens has been observed in systems such as the anterior-posterior patterning of the vertebrate limb, the dorsal-ventral patterning of the vertebrate neural tube, the axes in Xenopus, and the leg and wing imaginal discs of *Drosophila*. Known morphogens include sonic Hedgehog (shh), which provides a graded signal for pattern formation in the ventral neural tube [24]; the transforming growth factor beta (TGF-beta) family, which is involved in dorsal-ventral patterning [109, 110]; retinoic acid, which stimulates growth of the posterior end of the organism [48]; and decapentaplegic (Dpp) and Wingless (Wg), which regulate patterning and growth in *Drosophila* leg and wing imaginal discs [3, 90, 112, 114]. More examples of specific biological functions for various morphogens can be found in other reviews [39, 111, 134, 130].

Aside from patterning, how morphogen gradients regulate tissue growth is also a critically important question in morphogen systems [3, 19, 23, 101, 130]. For example, the *Drosophila* wing disc begins with approximately 40 cells and reaches a size of 50,000 cells in the late third instar larva [69]. Recent experimental studies on the development of the *Drosophila* wing disc indicate that growth will not occur without morphogens; however, cell proliferation is found to be spatially uniform in the wing disc, even with a spatially graded morphogen [81]. This peculiar result raises the question of how the spatially inhomogeneous morphogen gradient is translated into uniform growth and how the wing disc maintains a robust final size at the end of development.

3. Reaction-diffusion equations driven by localized sources: morphogen gradient formation

A number of mathematical models have been proposed for studying the formation of morphogen gradients. Most of the models consist of morphogen diffusion and the interaction among morphogen and cellular molecules, and hence, the model of reaction-diffusion equations is a basic framework for understanding this biological system [55, 128]. Here, we mainly focus on the formation of long-range morphogen gradients (for example, the Dpp gradient in the *Drosophila* wing imaginal disc shown in Fig. 2A) and review some mathematical models that were developed from the study of morphogen gradient formation, robustness, and growth control.

3.1. Ligand diffusion in extracellular space

The simplest biologically possible model is shown in Fig. 2B. In this model, diffusive ligands are sythesized at a local site and then reversibly bind to receptors to form signaling complexes, and the signaling complexes are endocytosed and degraded. In many situations, the morphogen activities essentially vary only in the direction perpendicular to the axis of the production region. This behavior leads to the following one dimensional reaction-diffusion equation of *ligand extracellular diffusion* (LED) (model B in [57]):

LED:

$$\frac{\partial[\mathrm{L}]}{\partial t} = V(X) + D\frac{\partial^2[\mathrm{L}]}{\partial X^2} - k_{\mathrm{on}}[\mathrm{L}](R_{\mathrm{tot}} - [\mathrm{LR}]) + k_{\mathrm{off}}[\mathrm{LR}], \tag{1}$$

$$\frac{\partial[\mathrm{LR}]}{\partial t} = k_{\mathrm{on}}[\mathrm{L}](R_{\mathrm{tot}} - [\mathrm{LR}]) - k_{\mathrm{off}}[\mathrm{LR}] - k_{\mathrm{deg}}[\mathrm{LR}]. \tag{2}$$

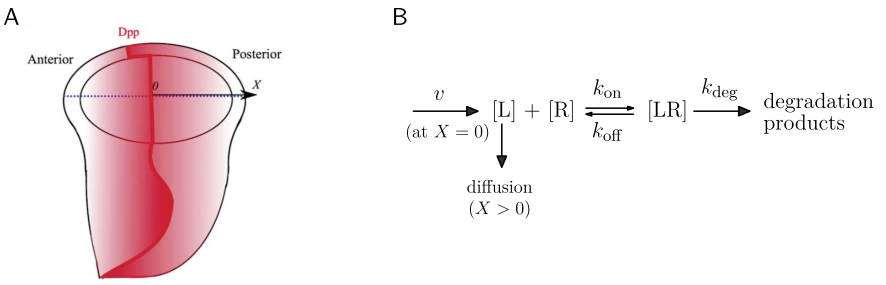

Figure 2: A simple diffusion model. (A) Illustration of the distribution of Dpp, shown in red, in the *Drosophila* wing imaginal disc. (B) The model with diffusion, reversible binding, and degradation (replotted from [57]). (Color figure online.)

Here, $0 \leq X \leq X_{\max}$ for one half of the tissue region; [L] and [LR] represent the concentration of ligands and signaling complexes, respectively; and the total receptor concentration is assumed to be a constant, $R_{\text{tot}} = [\text{R}] + [\text{LR}]$. The formation and dissociation rates of the ligand-receptor complexes are k_{on} and k_{off}, respectively, and the degradation rate of the signaling complexes is k_{deg}. The diffusion is assumed to be governed by Fick's second law, with D the diffusion coefficient. The ligand production region along tissue cells is specified by the function $V(X)$. The localized synthesis site is often represented by a narrow region of finite width $0 \leq X \leq X_{\min}$. Thus, the production rate $V(X)$ is given in terms of the *Heaviside unit step function* $H(z)$ (referred to [63, 64]):

$$V(X) = \frac{v}{X_{\min}} H(X_{\min} - X), \qquad H(z) \equiv \begin{cases} 0, & (z < 0) \\ 1, & (z \geq 0) \end{cases}. \tag{3}$$

Here v is the synthesis rate per unit length. The no-flux condition is often assumed at the one side of the morphogen production

$$\frac{\partial [\text{L}]}{\partial X} = 0 \quad \text{at} \quad X = 0, \tag{4}$$

as a consequence of the symmetry relative to the border. At the other end of the production, a sink condition is often used so that:

$$[\text{L}] = 0 \quad \text{at} \quad X = X_{\max}. \tag{5}$$

For simplicity, we often consider the situation of point source, where the ligand is only produced at $X = 0$. To this end, we can take the limit $X_{\min} \to 0$ in (3); therefore, the production rate $V(X)$ is given as a delta function

$$V(X) = v\delta(X). \tag{6}$$

We note that the boundary condition (4) is not valid in this case.

In the case of a point source, mathematical analysis shows that the steady state gradient of the LED model depends on only two dimensionless parameters, the ligand *synthesis-to-degradation ratio* β and the *effective on rate* ψ, which are defined as

$$\beta = \frac{v}{R_{\text{tot}} k_{\text{deg}}}, \quad \psi = \frac{X_{\max}^2 k_{\text{deg}}}{D} \frac{k_{\text{on}} R_{\text{tot}}}{(k_{\text{off}} + k_{\text{deg}})}. \tag{7}$$

A biologically useful gradient (i.e., able to broadly distribute patterning information over the entire field of cells) can be produced only when $\beta < 1$ and

the combination of β and ψ take values from a particular region [57]. For biological gradients, the resulting signaling gradient exponentially decays from the production border toward the other end. Linear stability analysis showed that the steady state gradients are asymptotically stable [79]. When a narrow region of ligand production is explicitly considered, it has been proved that the system with a narrow region of ligand production always has a positive steady state morphogen gradient, and hence there is no restriction on the synthesis-to-degradation ratio for the existence of steady state gradient [63].

The idea that an in vivo morphogen gradient is formed by diffusion was rejected in an early study by [50]. In this study, morphogen diffusion was simulated over 180 receptor-bearing cells and the authors concluded that morphogens can saturate all receptors in a region of tissue and thus cannot form a biologically useful signaling gradient. However, this negative conclusion was based on a numerical scheme without the degradation of signaling molecules, which corresponds to the situation of $k_{\text{deg}} = 0$ (i.e., $\beta = +\infty$) in the LED model. Hence, this simulation would not exclude the diffusive mechanism of gradient formation. The analysis in [57] further clarified the condition to allow biologically useful gradients when $\beta < 1$. These results highlighted the importance of qualitative study in understanding experimental facts [34].

The basic model (1)–(2) has been refined in many studies for more realistic situations, including the distributed synthesis of receptors [63, 79], endocytosis and exocytosis of receptors and signaling complexes [57, 79], and extensions to two- or three-dimensional diffusion [123]. These improvements make little difference to the conclusion of morphogen gradient formation but can be more difficult in terms of mathematical analysis.

Despite the formation of biological gradients, numerical simulations have showed that the signaling gradients produced from the above diffusion mechanism are not robust enough with respect to changes in the system parameters, as small changes in the ligand production rate can cause substantial changes in the gradient shape [57]. In contrast, embryonic patterning is usually highly robust, resisting not only substantial changes in the expression level of individual genes but also fluctuating environmental conditions. These results suggest that additional biological processes must be at work to ensure such robustness, leading to further model improvements that are reviewed below. The contributions to robustness are discussed in Section 4.

3.2. Self-enhanced ligand degradation

In [28], the authors proposed the idea that self-enhanced ligand degradation can enhance the robustness of morphogen gradients. In this case, the

degradation of morphogens is formulated as a nonlinear function of its own concentration, instead of a linear function by first order degradation. A simple aspect of *self-enhanced ligand degradation* (SED) can be seen from the following diffusion equation with a power-law degradation profile

$$\textbf{SED}: \qquad \frac{\partial[\mathrm{L}]}{\partial t} = D\frac{\partial^2[\mathrm{L}]}{\partial X^2} - \alpha[\mathrm{L}]^n + v\delta(X). \tag{8}$$

In the case of linear degradation ($n = 1$), the steady state gradient is exponential decaying (here we assume the approximation $X_{\max} \to +\infty$) (also see [52])

$$[\mathrm{L}] = [\mathrm{L}]_0 e^{-X/\Delta_d}, \quad [\mathrm{L}]_0 = v/\alpha, \quad \Delta_d = \sqrt{D/\alpha}. \tag{9}$$

It is obvious that the steady state concentration is linearly dependent on the ligand production rate; thus the morphogen gradient linearly tracks the changes of the production rate when there are external perturbations to ligand synthesis.

In the case of nonlinear degradation ($n > 1$), the steady state gradient is power-law decaying (referred to [36] for detailed analysis):

$$[\mathrm{L}] = \frac{[\mathrm{L}]_0}{(X/\varepsilon + 1)^m}, \quad [\mathrm{L}]_0 = \sqrt[n]{v/\alpha}, \quad m = \frac{2}{n-1}, \ \varepsilon = \sqrt{\frac{Dm(m+1)}{\alpha L_0^{n-1}}}. \tag{10}$$

Now, the steady state concentration depends on the ligand production rate in a sublinear way, and hence, the morphogen gradient can buffer against the fluctuations in the production rate.

Biologically, self-enhanced ligand degradation can be achieved through a morphogen network composed of morphogen signaling-regulated (enhanced or repressed) receptor expression and receptor-mediated ligand degradation (often through a protease). Two types of regulation were proposed in [28]: the Wingless(Wg)-like class, in which morphogen signaling represses the receptor and the receptor stabilizes the morphogen, and the Hedgehog(Hh)-like class, in which morphogen signaling activates receptor expression, and the receptor enhances morphogen degradation. A general formulation is given by the following set of reaction-diffusion equations [28]:

$$\begin{aligned} \frac{\partial[\mathrm{L}]}{\partial t} = {} & V(X) + D\frac{\partial^2[\mathrm{L}]}{\partial X^2} - k_+^1[\mathrm{L}][\mathrm{R}] + k_-^1[\mathrm{LR}] \\ & - a_1[\mathrm{PR}][L] - a_2[\mathrm{P}][\mathrm{L}] - a_3[\mathrm{L}], \end{aligned} \tag{11}$$

$$\frac{\partial[\mathrm{LR}]}{\partial t} = k_+^1[\mathrm{L}][\mathrm{R}] - k_-^1[\mathrm{LR}] - a_4[\mathrm{LR}], \tag{12}$$

SED':
$$\frac{\partial[\mathrm{PR}]}{\partial t} = k_+^2[\mathrm{R}][\mathrm{P}] - k_-^2[\mathrm{PR}], \tag{13}$$

$$\begin{aligned}\frac{\partial[\mathrm{R}]}{\partial t} &= \eta_{r1}\frac{K_a^m}{K_a^m + [\mathrm{LR}]^m} + \eta_{r2}\frac{[\mathrm{LR}]^n}{K_b^n + [\mathrm{LR}]^n} - k_+^2[\mathrm{R}][\mathrm{P}] \\ &\quad + k_-^2[\mathrm{PR}] - k_+^1[\mathrm{R}][\mathrm{L}] + k_-^1[\mathrm{LR}] - \alpha_5[\mathrm{R}] + \rho\alpha_4[\mathrm{LR}],\end{aligned} \tag{14}$$

$$[\mathrm{P}] = P_{\mathrm{tot}} - [\mathrm{PR}], \tag{15}$$

where [L], [R], and [P] denote the concentrations of the ligand, receptor, and protease, respectively, and the complexes are denoted by their constituents. Different types of Wg-like or Hh-like regulation can be defined by adjusting the parameters for protease-mediated ligand degradation (a_1 and a_2) and for receptor expression (η_{r1} and η_{r2}).

3.3. Non-receptor mediated ligand transport

Morphogen gradient formation may be modulated by interactions with heparan sulfate proteoglycans (HSPGs) and other extracellular proteins that tether morphogens to the cell surface [4, 8, 40, 53, 113, 137]. Such non-signaling entities are called *non-receptors* because they bind with morphogens in a way similar to receptors, but the resulting complexes do not signal cell fate decisions. A good introduce was provided in [54] for how HSPGs affect the stability and distribution of extracellular gradients. Many experiments have shown that non-receptors play an important role in the formation and robustness of morphogen gradients, such as Dpp, Wg, and Hh [40, 74, 82, 137].

The basic model in Section 3.1 can be extended to include the binding of morphogens with non-receptors, as illustrated in Fig. 3. In this model, we consider a fixed concentration N_{tot} of proteoglycan-type non-diffusive non-receptors and introduce a set of similar activities for the non-receptor sites. These assumptions yield the following set of reaction-diffusion equations of *non-receptor mediated ligand extracellular diffusion* (N-LED), described in [66]:

$$\begin{aligned}\frac{\partial[\mathrm{L}]}{\partial t} &= V(X) + D\frac{\partial^2[\mathrm{L}]}{\partial X^2} - k_{\mathrm{on}}[\mathrm{L}](R_{\mathrm{tot}} - [\mathrm{LR}]) \\ &\quad + k_{\mathrm{off}}[\mathrm{LR}] - j_{\mathrm{on}}[\mathrm{L}](N_{\mathrm{tot}} - [\mathrm{LN}]) + j_{\mathrm{off}}[\mathrm{LN}],\end{aligned} \tag{16}$$

N-LED:
$$\frac{\partial[\mathrm{LR}]}{\partial t} = k_{\mathrm{on}}[\mathrm{L}](R_{\mathrm{tot}} - [\mathrm{LR}]) - (k_{\mathrm{off}} + k_{\mathrm{deg}})[\mathrm{LR}], \tag{17}$$

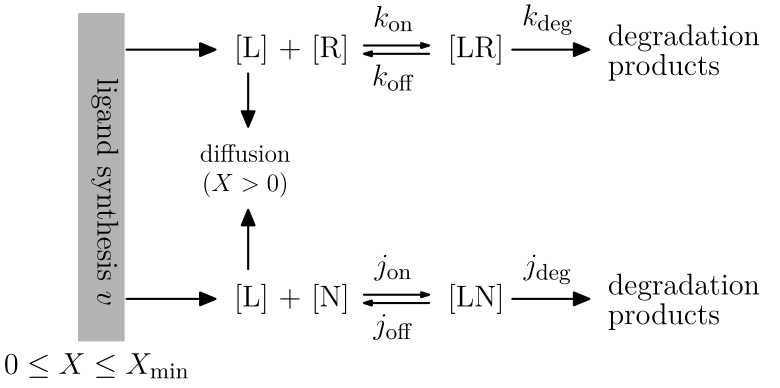

Figure 3: Illustration of the non-receptor mediated morphogen gradient formation.

$$\frac{\partial[\mathrm{LN}]}{\partial t} = j_{\mathrm{on}}[\mathrm{L}](N_{\mathrm{tot}} - [\mathrm{LN}]) - (j_{\mathrm{off}} + j_{\mathrm{deg}})[\mathrm{LN}]. \tag{18}$$

Here, [LN] represents the concentration of ligand-non-receptor complexes, $N_{\mathrm{tot}} = [\mathrm{N}] + [\mathrm{LN}]$, and the other variables are the same as in the above LED model. Similarly to the discussions in Section 3.1, the ligand production region is specified at $0 \leq X \leq X_{\mathrm{min}}$, and the ligand production rate $V(X)$ is taken as a delta function $V(X) = v\delta(X)$ for a point source ($X_{\mathrm{min}} = 0$) or a step function $V(X) = (v/X_{\mathrm{min}})H(X_{\mathrm{min}} - X)$ if $X_{\mathrm{min}} > 0$.

The existence, uniqueness, and linear stability of the steady state gradient for the N-LED model were analytically studied in [66]. Similarly to the case without non-receptor, when $X_{\mathrm{min}} = 0$ (point source), the system has a unique steady state gradient if the synthesis-to-degradation ratio, now defined as

$$\beta = \frac{v}{R_{\mathrm{tot}}k_{\mathrm{deg}} + N_{\mathrm{tot}}j_{\mathrm{deg}}}, \tag{19}$$

satisfies $\beta < 1$. When $X_{\mathrm{min}} > 0$ (narrow production region), the system always has a unique steady state gradient. Furthermore, the steady state gradient is linearly stable in either of these situations. The presence of non-receptor should reduce the amount of morphogen available for binding to receptors and thereby inhibit cell signaling. This aspect was analytically proved in [66]: for sufficiently low morphogen synthesis rates, the presence of non-diffusive non-receptors generally lowers the normalized concentration level of both free ligand and ligand-receptor concentrations at each point

of the solution domain, reduces the steepness of the negative slope, and increases the convexity of the concentrations (see Theorem 3 in [66]).

Although the system always has a steady state gradient when $X_{\min} > 0$, not all gradient shapes are biologically useful, i.e., some gradients may not be *multi-fate gradients* that can broadly distribute patterning information over the entire field of cells. In [72], the multi-fate gradient was defined in a mathematical way based on the following three aspects of the gradient profile: the slope of the normalized signaling gradient should not be too steep; the concentration of patterning signal should not be too low in the vicinity of the ligand production region; and the slope of the normalized free ligand concentration at the farther end of the tissue should be a small value. Analysis of the model equation showed that the steady state gradient mainly depends on four parameters [72]: the normalized ligand synthesis rate v, the ratio of saturation levels of receptors to non-receptors γ, the ratio of degradation flux of receptors to non-receptors p, and the total degradation flux of receptors and non-receptors λ. Furthermore, when γ is small enough, a multi-fate gradient can be achieved for a suitable level of the ligand synthesis rate v. These results outline the restrictions to produce a biologically acceptable multi-fate gradient following the N-LED model.

Most HSPGs are static components in the extracellular matrix and therefore are considered to be non-diffusible. However, these non-diffusible non-receptors can transport ligands through a "bucket brigade" pathway to form long-range signals [71, 70, 73] (restricted diffusion model in [137]) (Fig. 4). With these "bucket brigade" transports, ligands move across the tissue in a manner similar to diffusion through the random work of the heparan sulfate (HS) chains and hence can again be mathematically described by diffusion equations [71]. Thus, we have a set of reaction-diffusion equations in which both [L] and [LN] are allowed to diffuse (N_D-LED, the N-LED with diffusion in non-receptors)[73]:

$$\frac{\partial[\mathrm{L}]}{\partial t} = V(X) + D_{\mathrm{L}}\frac{\partial^2[\mathrm{L}]}{\partial X^2} - k_{\mathrm{on}}[\mathrm{L}][\mathrm{R}] + k_{\mathrm{off}}[\mathrm{LR}] - j_{\mathrm{on}}[\mathrm{L}](N_{\mathrm{tot}} - [\mathrm{LN}]) + j_{\mathrm{off}}[\mathrm{LN}] - k_{\mathrm{deg,L}}[\mathrm{L}], \tag{20}$$

$$\textbf{N}_{\mathbf{D}}\textbf{-LED}: \quad \frac{\partial[\mathrm{R}]}{\partial t} = \omega_R([\mathrm{LR}]) - k_{\mathrm{on}}[\mathrm{L}][\mathrm{R}] + k_{\mathrm{off}}[\mathrm{LR}] - k_{\mathrm{deg,R}}[\mathrm{R}], \tag{21}$$

$$\frac{\partial[\mathrm{LR}]}{\partial t} = k_{\mathrm{on}}[\mathrm{L}][\mathrm{R}] - (k_{\mathrm{off}} + k_{\mathrm{deg,LR}})[\mathrm{LR}], \tag{22}$$

$$\frac{\partial[\mathrm{LN}]}{\partial t} = D_{\mathrm{LN}}\frac{\partial^2[\mathrm{LN}]}{\partial X^2} + j_{\mathrm{on}}(N_{\mathrm{tot}} - [\mathrm{LN}]) - (j_{\mathrm{off}} + j_{\mathrm{deg}})[\mathrm{L}]. \tag{23}$$

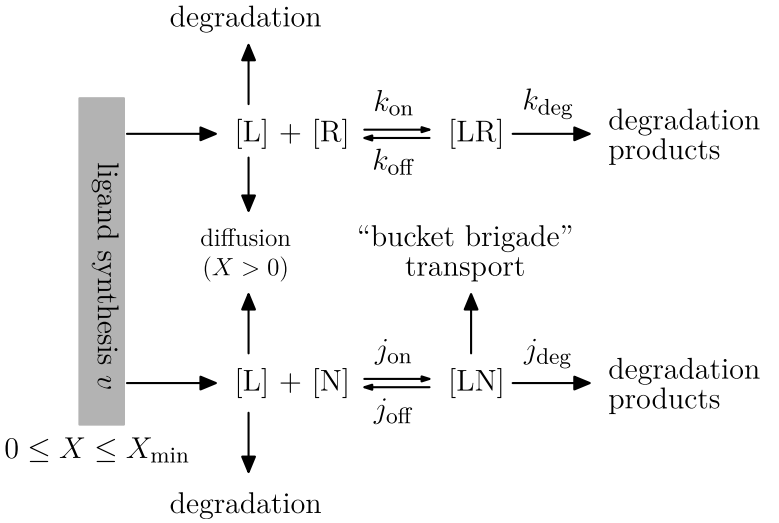

Figure 4: The model of morphogen gradient formation with "bucket brigade" transport through membrane-associated non-receptors and possible fast degradation of free ligands.

Here, the synthesis and degradation of receptors are explicitly included, and feedback from the signaling molecule to receptor synthesis is given by the function ω_R. Furthermore, the degradation of free ligand, with a degradation rate $k_{\mathrm{deg,L}}$, is also included. If the morphogen is rapidly turned over ($k_{\mathrm{deg,L}} \gg j_{\mathrm{on}} N_{\mathrm{tot}}$) but is protected against degradation while binding to the non-receptors ($j_{\mathrm{deg}} = 0$), the system has a unique steady state solution, and the solution is linearly stable [73].

In several studies of the formation of the BMP gradient in *Drosophila* or zebrafish embryos [78, 85, 105, 139], the binding of morphogen to the diffusible non-receptor can result in sharp enhancement of the signaling gradients. Mathematical models of these studies are similar to the above equations; however, the boundary conditions are different in that the tissue geometries are modeled as closed circles for the patterning of dorsal-ventral development.

3.4. Receptor-mediated transcytosis

In additional to the formation of long-distance gradients by free diffusion and/or "bucket brigade" transportation through non-receptors, the morphogen can also be transported with the help of receptors, a process termed

transcytosis, i.e., by repeated rounds of morphogen binding to cell surface receptors, internalization into the cell and subsequent externalization, and release of the ligand from the receptor on the cell surface (i.e., dynamin-dependent endocytosis) [16, 15, 14, 30, 92].

Similarly to the LED model in Section 3.1, a simple model of such *receptor-mediated transcytosis* (RMT) can be formulated as

$$\frac{\partial [\mathrm{L}]}{\partial t} = V(X) - k_{\mathrm{on}}[\mathrm{L}](R_{\mathrm{tot}} - [\mathrm{LR}]) + k_{\mathrm{off}}[\mathrm{LR}], \tag{24}$$

$$\textbf{RMT}: \quad \frac{\partial [\mathrm{LR}]}{\partial t} = D\frac{\partial^2 [\mathrm{LR}]}{\partial X^2} + k_{\mathrm{on}}[\mathrm{L}](R_{\mathrm{tot}} - [\mathrm{LR}]) - k_{\mathrm{off}}[\mathrm{LR}] - k_{\mathrm{deg}}[\mathrm{LR}]. \tag{25}$$

Discussions in [57] have shown that transcytosis can form a multi-fate gradient; however, a series of cell biological events would have to occur at implausibly fast rates to form the gradient in a reasonable timeframe.

In [15] and [14], based on a microscopic model of transcytosis transport, the authors derived effective transport equations and showed that transcytosis can lead to robust ligand profiles. Moreover, in [16], the authors further discussed the precision of a morphogen gradient by considering how cell-to-cell variability in the source, the target tissue, or both contribute to the variations of the gradient. In these studies, each single cell in the field of interest was considered individually, and the system dynamics can be described by a set of ordinary differential equations. Thus, cell-to-cell variability was modeled through fluctuations in the concentrations of intracellular and extracellular molecules and system parameters.

There has been a long debate regarding whether a long-range morphogen gradient is formed by morphogen diffusion or by non-diffusive mechanisms [50, 57, 92, 140]. In [52], kinetic parameters of two key morphogens, Decapentaplegic (Dpp) and Wingless (Wg), during the development of the fly wing were studied quantitatively. Dpp forms a longer-range gradient than Wg. The kinetic parameters suggested that dynamin-dependent endocytosis was required for the gradient formation of Dpp but not of Wg. However, the dynamin-dependent endocytosis of Dpp can be the result of ligands binding to either receptor or non-receptor, which yield different type formulations of diffusive ligand-receptor (the RMT model (24)–(25)) or ligand-non-receptor (the $\mathrm{N_D}$-LED model (20)–(23)). The receptor plays different roles in these two models. In the receptor-mediated transcytosis model, the receptor is essential for the endocytosis, re-secretion, and thus transport of ligands,

whereas in the ligand extracellular diffusion model, receptors merely modulate ligand distribution by binding the ligand at the cell surface for internalization and signaling. In [102], the authors combined genetic tools with mathematical modeling to discriminate between the two models for Dpp gradient formation in the *Drosophila* wing disc. They analyzed how receptor mutant clones affect the Dpp profile and suggested that receptor-mediated transcytosis cannot account for the Dpp gradient formation, and thus the Dpp gradient should be formed following the mechanism of extracellular diffusion mechanism [102].

3.5. Other models

In the above models, we mainly discuss gradient formations in which morphogens are sythesized at a localized site and transported to further tissue cells at the other side to form a long-range signaling gradient. The formulation of these gradients is usually modeled by reaction-diffusion equations with a source term at one side and a sink at the other side, and hence the signaling gradient at steady state is driven by the boundary conditions (the source term). Hence, the steady state pattern is described by a set of nonlinear boundary value problems, and a key mathematical question is to determine how the solution of the boundary value problem depends on system parameters. In most mathematical models, the positional information is assumed to be decoded by the concentration of signaling molecules at steady state. However, alternative decoding strategies are also possible, including pre-steady state readout [12], temporal derivatives of the morphogen concentration [98], dynamics of morphogen signaling [131, 129], and the integration of signals from multiple morphogens [83, 88].

There are many other biological problems that yield alternative forms of mathematical models. In the dorsal-ventral patterning of *Drosophila* embryonic development, the morphogens Dpp and short gastrulation (Sog) are synthesized in different regions, diffuse to the whole tissue, and then interact with each other to pattern tissue development [26, 67, 104]. A mathematical model of such Dpp/Sog patterning was developed in [78]. In this model, the *Drosophila* embryo was represented by a ring for the dorsal-ventral cross-section, Dpp is only produced in the upper part (dorsal region), and Sog is only produced in the lower part (ventral region). Hence, the steady state gradient is regulated by the interactions between the two morphogens. The effect of receptor over-expression in the Dpp-Sog system was discussed in [67]. A similar computational model, but in three spatial dimensions, was developed for the BMP gradients in the dorsal-ventral patterning of the zebrafish embryo [139].

In addition to the mechanisms of patterning with signaling gradients, other developmental patterning strategies include patterning with activator-inhibitor systems (i.e., Turing's theory), genetic oscillations in neighboring cells, or mechanical deformations. Refer to [55], [86] and [80] for reviews of the mathematical models and computational approaches of these patterning strategies.

How tissue growth affects the scaling of a morphogen gradient and how a morphogen gradient mediates tissue growth are interesting questions formulated in recent years. Mathematically, these questions lead to the scaling solution of reaction-diffusion equations and moving boundary problems, which are discussed in Section 5.

4. Robustness of morphogen gradients

Robustness — a phenotypic trait of the absence or low level of variation of phenotype in the face of genetic and/or environmental perturbation — has become a commonly used term in biological studies [32]. During embryonic development, there are many perturbations that can be unfavorable for precise pattern formation. Hence, it is important for an embryo to be tolerant toward different perturbations, including noisy environmental variation and genetic variation. Exploring the robustness of morphogen gradient formation and identifying ways of producing robust patterning has become a major research topic in recent years [61, 60, 117]. Most works have focused on parametric robustness, i.e., insensitivity to parameter values [27, 58, 61, 72, 73, 76, 87, 105, 124, 125, 132]. Some investigators also focus on the "precision" of morphogen gradients, i.e., the natural variation among individuals in a population [16, 29, 38, 45, 116]. Recently, a few studies have drawn attention to the effects of noise in morphogen gradients, especially the precision of patterning boundaries [16, 43, 44, 138].

The precise definition of robustness is often ambiguous, despite its common use in biological studies. When defining robustness, it is important to specify which trait is robust to which perturbation and to provide a quantification for measuring robustness [32]. The robustness of a system to external or internal variations is often quantified by the *sensitivity coefficient*, which corresponds to the fold change in the output of interest in response to a given fold change in a particular input [96].

For the morphogen gradient formations discussed in this review, often described by a set of reaction-diffusion equations with suitable boundary conditions, the signaling gradient is described by the solution of the resulting boundary value problem at steady state. Here, we introduce general ways

to define robustness. To this end, we always assume that the boundary value problem has a unique solution, denoted by $\mathrm{Sig}(X;p)$, and the signal concentration at position X is dependent on the parameter value p. Therefore, the sensitivity coefficient of the signal with respect to changes in p is defined as

$$S_{\mathrm{Sig},p}(X) = \left|\frac{\partial \ln \mathrm{Sig}}{\partial \ln p}\right| = \left|\frac{p}{\mathrm{Sig}}\frac{\partial \mathrm{Sig}(X;p)}{\partial p}\right|. \tag{26}$$

This sensitivity coefficient is based on the definitions for robustness in many studies, such as [15, 28, 71, 73].

In experiments, a natural pattering phenotype is to measure the location X of cells with a particular cell type, which is determined by the corresponding signaling level Sig. Thus, as in [76], the corresponding sensitivity coefficient is given by

$$S_{X,p}(\mathrm{Sig}) = \left|\frac{p}{X}\frac{\partial X(\mathrm{Sig},p)}{\partial p}\right|. \tag{27}$$

When the cell type is well defined by a signaling threshold, the robustness of patterning can be measured by the sensitivity coefficient at the signaling boundary, i.e., $S_{X,p}$ with signaling concentration taken as the threshold value. Otherwise, the robustness of patterning formation with respect to the parameter p can be defined as the mean of sensitivity over the signaling region

$$R_p = \frac{1}{\mathrm{Sig}_1 - \mathrm{Sig}_0}\int_{\mathrm{Sig}_0}^{\mathrm{Sig}_1}\left|\frac{p}{X}\frac{\partial X(\mathrm{Sig},p)}{\partial p}\right| d\,\mathrm{Sig}. \tag{28}$$

The sensitivity coefficient defined by (27) is a good quantity to measure the variation with respect to small changes in the input parameter, i.e., perturbations in system parameters. However, in biological systems, mutations in genes can yield significant changes to certain parameters, such as protein synthesis rates [87]. To measure the robustness with respect to these changes, the root-mean-square of cell displacement after parameter changes would be a meaningful measurement of robustness, which is formulated as [72]

$$R_{p\to p'} = \frac{1}{|X(\mathrm{Sig}_1,p) - X(\mathrm{Sig}_0,p)|}\sqrt{\frac{1}{\mathrm{Sig}_1 - \mathrm{Sig}_0}\int_{\mathrm{Sig}_0}^{\mathrm{Sig}_1}(\Delta X)^2 d\,\mathrm{Sig}}, \tag{29}$$

where $\Delta X = X(\mathrm{Sig},p') - X(\mathrm{Sig},p)$ is the change in cell location, with a given signaling concentration Sig, when p is changed to p'.

The above definitions are straightforward for parametric robustness in which changes in parameters often shift the signaling gradient in a single direction. However, the boundary between different cell fates is well defined by the concentration threshold, whereas noise perturbations in cell-to-cell variations can often mix up the cell fate boundary and induce a "salt-and-pepper" transition zone. In this situation, a *sharpness index* is often defined for the robustness of patterning formation in the context of noise perturbations [76, 77, 138].

Mathematically, the formulation of the steady state solution demonstrates that this robustness (or sharpness index) depends on the system parameters in a highly nonlinear way. Hence, it is difficult to perform mathematical analysis of the robustness dependence. Below, we introduce two typical examples to discuss the mathematical questions that arise from robustness analysis.

4.1. A boundary value problem: perturbation in morphogen synthesis

We begin by reviewing a well-accepted strategy for achieving parametric robustness in morphogen gradients: the principle of self-enhanced clearance [28]. A simple model to demonstrate how a morphogen's stimulation of its own degradation can provide a way to build a robust gradient is described in Section 3.2. From equation (8), in the case of linear degradation ($n = 1$), the sensitivity of the ligand concentration at X with respect to the concentration at the synthesis site is

$$S_{X,L_0}|_{n=1} = \left| \frac{L_0}{[\mathrm{L}]} \frac{\partial [\mathrm{L}]}{\partial L_0} \right| = 1. \tag{30}$$

When there is self-enhanced clearance ($n > 1$), the sensitivity coefficient is given by

$$S_{X,L_0}|_{n>1} = 1 - \frac{X/\varepsilon}{X/\varepsilon + 1}. \tag{31}$$

Thus, self-enhanced clearance (increasing n) tends to decrease the sensitivity of ligand concentration to variation in the morphogen synthesis, hence improving robustness. Refer to [61] for a review of the strategy of self-enhanced clearance.

A possible means of self-enhanced clearance can be the consequence of enhancing ligand degradation through non-signaling receptors (non-receptor).

Analytical studies in [72] provided a theoretical basis of how a robust signaling gradient can be achieved by substantial binding of the signaling morphogen to non-receptors and degradation of the resulting complexes at a sufficiently rapid rate. A simple model of morphogen gradient formation including the reversible binding and unbinding of ligands with non-receptors and the rapid degradation of the resulting complexes is shown by (16)–(18) (the N-LED model) in Section 3.3. Alternatively, see [72] for a model including the synthesis of the receptor and non-receptor and the transport of extra- and intracellular molecules. To analyze the robustness, the dimensionless form of the steady state equation for the normalized free ligand concentration $a(x)$ can be written as follows [72]:

$$a'' - \lambda^2 \left(\frac{p}{1+a} + \frac{1-p}{1+\gamma a} \right) a + (v/d) H(d-x), \quad (\ )' = \frac{d(\ )}{dx}, \tag{32}$$

where $0 < x < 1$ is the normalized spatial variable, H is the Heaviside unit step function so that the ligand synthesis region is limited to $[0, d]$, and the boundary condition is defined as

$$a'(0) = a(1) = 0. \tag{33}$$

The normalized concentration of the signaling morphogen-receptor complexes is given by

$$b(x) = \frac{a(x)}{a(x)+1}. \tag{34}$$

Hence, the signaling gradient $b(x)$ is defined by the boundary value problem (32)–(34). There are five dimensionless parameters: the relative width of the ligand production region d, the normalized ligand synthesis rate v, the ratio of the saturation level of receptors to the saturation level of non-receptors γ, the ratio of the degradation fluxes of the receptor to the degradation fluxes of the non-receptor p, and the sum of these fluxes λ^2. Here, d is a geometric parameter and is often fixed in studies (for example, $d = 0.06$ in the case of the *Drosophila* wing imaginal disc, corresponding to the width of 12μm for the production region compared with the total width of 200μm), and hence the signaling gradient and robustness depend on the other four parameters: v, γ, p, λ. Here, we note that $p = 1$ corresponds to the situation without non-receptor. Given the nonlinear boundary value problem, the dependence of the signaling concentration on parameters is not obvious, and hence it is not straightforward to calculate the robustness.

Using the energy integral method, it has been shown that the boundary value problem (32)–(33) has a unique solution, and hence the robustness measures how sensitively this unique solution depends on system parameters. The robustness with respect to a 2-fold change in the synthesis rate ($v \to 2v$) was discussed in [72], in which the robustness index R was defined by the root-mean-square of cell displacement (29). Focusing at multi-fate signaling gradients, it was proven that the robustness has a lower bound defined by a function $J(p, \gamma)$:

$$J(p,\gamma) = \min_{\xi>0} \frac{\int_{\xi}^{2\xi} \frac{du}{\sqrt{E(u)}}}{\int_{\frac{\xi}{5+4\xi}}^{\xi} \frac{du}{\sqrt{E(u)}}}, \quad E(u) = \int_0^u a\left(\frac{p}{1+a} + \frac{1-p}{1+\gamma a}\right) da. \tag{35}$$

In particular, when $p = 1$ (the case without non-receptor), $J(1, \gamma) > 0.35$, which indicates that without non-receptor, the system always has poor robustness (biologically acceptable robustness is often taken to be $R < 0.2$). This analysis provided a theoretical base for the numerical simulation studies in [65] of the nonexistence of robust multi-fate gradients without non-receptors among simulations conducted for 2^{20} random sets of parameter values. In the opposite situation, when $p = 0$ (the case without receptor) and $\gamma = 0$, the boundary value problem (32)–(33) can be solved explicitly, and good robustness can be achieved if the ligand synthesis rate v is large enough. Despite the biologically non-realistic situation $p = 0$, based on the continuous dependence of the robustness R on the four parameters p, γ, λ, v, good robust multi-fate gradients are possible if both p and γ are small values and v is large enough. Biologically, these conditions are met as follows: (1) a receptor degradative flux sufficiently low relative to the non-receptor and (2) the synthesis rate of free ligand is sufficiently high, but not high enough to saturate available receptors in signaling cells [72].

As discussed previously, the formation of a morphogen gradient can also be modeled by "bucket brigade" transportation so that free ligands move long distances through the help of non-receptors, which results in the N_D-LED model (20)–(23). The normalized steady state gradient is given by the following boundary value problem [73]:

$$\theta_l \frac{\partial^2 l}{\partial x^2} - (l - w) - \varepsilon\left(l\,(1 - w) - \gamma\,(\alpha\, u - l\, r)\right) + (\eta/\varepsilon) H(d - x) = 0, \tag{36}$$

$$\frac{\partial^2 w}{\partial x^2} - \lambda^2 (w - \varepsilon\, l\,(1 - w)) = 0, \tag{37}$$

where $0 < x < 1$, the functions u and r depend on l through

$$l = (\alpha + 1)u/r, \quad r = k(u) - \mu u. \tag{38}$$

Here, l and u are normalized ligand and ligand-non-receptor complex concentrations, respectively, and u is the normalized signaling (ligand-receptor complex) concentration. The boundary conditions are

$$w'(0) = l'(0) = w(1) = l(1) = 0, \quad (\ )' = \frac{d(\ )}{dx}. \tag{39}$$

The nonlinear function $k(u)$ represents the feedback from signal concentration to the synthesis of receptors. Non-positive feedback is often considered, so that

$$k(0) = 1, k'(u) \leq 0, k(u) > 0, \quad \forall u \geq 0. \tag{40}$$

To study robustness with respect to the ligand synthesis rate, we need to investigate how the solution $u(x)$ of the above boundary value problem depends on η. In [73], it was proven that if ε is small enough, then a unique combination of biologically acceptable gradients $\{w, (x), l(x), u(x), r(x)\}$ exist, i.e., the gradients satisfy (36)–(38), and the restrictions

$$0 \leq w(x) \leq 1, l(x) \geq 0, r(x) \geq 0, u(x) \geq 0, (0 \leq x \leq 1). \tag{41}$$

When $\varepsilon \ll 1$ and $\theta_l \ll 1$, the approximation of the acceptable gradients can be calculated explicitly. Based on these approximations, [73] discussed the robustness of the signaling gradient when the ligand synthesis rate η increases to η', $R_{\eta \to \eta'}$, and showed that $R_{\eta \to \eta'} = O(\eta^{-1/2})$ when η is sufficiently large. This result suggests that a robust gradient can be achieved for a high ligand synthesis rate. Biologically, the conditions $\varepsilon \ll 1, \theta_l \ll 1$ and $\eta \gg 1$ are met if (1) the free ligand is rapidly turned over and (2) the ligand synthesis rate is large enough that non-receptors in the ligand production region have high occupancy.

Cell membrane non-signaling receptors (such HSPG) are important for the formation of morphogen gradients. A series of studies have shown that the presence of non-receptors is favorable for robust gradients [71, 72, 73]. The desired robust morphogen gradient with respect to substantial perturbations of the morphogen synthesis rate is seen to be achievable through two different mechanisms involving regulation by non-receptors [73]:

Mechanism 1: Substantial (reversible) binding of slowly turned over morphogen molecules with membrane-bound non-receptors, with the resulting non-signaling complexes degrading at a sufficiently rapid rate.

Mechanism 2: Fast binding of rapidly turned over free morphogen molecules with non-receptors so that the non-signaling complexes move downstream through a "bucket brigade" process.

However, the above two mechanisms fail to generate good robustness with respect to perturbations in the receptor synthesis rate due to the restriction of the kinetic and diffusive resistances in molecule transportation [71, 76]. As a consequence of this restriction, there is a trade-off between the robustness with respect to the receptor synthesis rate and the signaling length scale. Hence, some other mechanisms must be involved to achieve robustness with respect to multiple perturbations.

In [76], the authors investigated the interplay between the robustness of patterning to the changes in receptor synthesis and morphogen synthesis and to the effects of cell-to-cell variability. Based on a simple model of morphogen gradient formation with diffusion and receptor-mediated uptake, the analysis showed the trade-offs and constraints to achieve these three performance objectives simultaneously. This study proposed a potential mechanisms for mitigating such trade-offs and constraints. The strategy includes the down-regulation of receptor synthesis in the morphogen source and the presence of non-receptors. Recently, the effects of feedback mechanisms on the robust gradient were discussed in [56]. In particular, a new approach to robust signaling gradients was introduced through nonlocal feedback with delay to the ligand synthesis rate [56, 108].

4.2. Stochastic modeling: cell-to-cell variability and noise in downstream

Cell-to-cell variation can be important for the precision of a morphogen gradient [44, 61, 136]. A simple diffusion-based model including cell-to-cell variation is described by [16] as

$$\frac{\partial}{\partial t}c(t,\vec{x}) = \nabla\cdot[(D_0+\eta(\vec{x}))\nabla c(t,\vec{x})] - (k_0+\xi(\vec{x}))c(t,\vec{x}), \tag{42}$$

where $c(t,\vec{x})$ is the ligand concentration, and $\vec{x}$ is a spatial position ($\vec{x} = (x,y)$ for 2 or $\vec{x} = (x,y,z)$ for 3 dimension). Here, $\eta(\vec{x})$ and $\xi(\vec{x})$ are random functions with zero average that describe the fluctuations in the diffusion

rate and clearance rate, respectively. The ligand synthesis is given by the boundary condition

$$(D_0 + \eta(\vec{x}))\frac{\partial}{\partial x}c(\vec{x},t) = -j_0 - \chi(\vec{x})|_{x=0}, \tag{43}$$

where j_0 is the average current across the boundary and $\chi(\vec{x})|_{x=0}$ is a random function with zero average.

Equation (42) describes morphogen gradient formation with cell-to-cell variation through a reaction-diffusion equation with spatially dependent coefficients. Due to the presence of multiplicative noise, the analytical calculation of the steady state solution is challenging. Numerical simulations in [16] showed that when there is cell-to-cell variability in the source, while the target cells are identical, the uncertainty of the morphogen concentration in the target tissue decreases with distance from the source. Alternatively, when the producing cells are identical but there is variability in the target, the uncertainty increases at large distances. In general, cell-to-cell variability exists in both the source and the target tissue. In this scenario, the uncertainty first decreases for a small distance from the source, reaches a minimum, and then increases for large distances. Hence, there is an optimal distance from the source at which the morphogen concentration has the best precision.

In pattern formation, cells sense their positions along morphogen gradients and collectively respond to form precise domains for target gene expression. However, noise perturbation can often affect the boundary in multi-fate cell patterning. Spatially constrained stochastic models suggest that noise depends predominantly on the transcription and translation dynamics of target gene expression [44], and external fluctuations in signals also play an important role in downstream responses [43]. Additionally, computational analysis of a stochastic model showed that noise could promote the sharpening of boundaries between adjacent segments [138].

In [138], the authors showed how noise drives the sharpening of gene expression boundaries in the development of rhombomeres in the zebrafish hindbrain, in which the morphogen retinoic acid (RA) induces the expression of *hoxb1a* in rhombomere 4 (r4) and *krox20* in r3 and r5. In this study, spatial and temporal noises in the morphogen synthesis and ligand-receptor binding were introduced to the reaction-diffusion model of RA morphogen gradient formation, and temporal noises were introduced for each gene expression. In the model, the two genes *hoxb1a* and *krox20* inhibit each other to form positive feedback, which yields bistability with either low or high expression of each gene. The temporal noise in gene expression can induce switches between the two expression states to form the patterning of the

zebrafish hindbrain. Computational analysis further showed that the spatial temporal noise in morphogen gradient formation can improve the sharpening of boundaries. This finding suggested a noise attenuation mechanism that relies on intracellular noise to induce switching and coordinate cellular decisions during developmental patterning [138].

5. Morphogen-mediated growth control

The morphogen gradient is closely related to tissue growth. To determine how the inhomogeneous morphogen gradient is translated into uniform growth and how the wing disc maintains a robust final size at the end, a number of potential growth control models have been proposed, including the temporal dynamics model [6, 130, 131], the slope model [100], the mechanical feedback model [1, 2, 106], and others. In the slope model, the relative slope of the signal controls cell division; in the temporal dynamics model, growth is regulated by the percentage of increase in the signal over time; and in the mechanical feedback model, the mechanical stress induces cell proliferation, while the final size of the tissue is controlled by the mechanical compression. However, the mechanisms for morphogen-mediated growth control remain controversial, as none of them can explain all significant biological data.

5.1. Scale-invariance of reaction-diffusion: scaling with tissue size

Scaling of the morphogen gradient with tissue size is essential for ensuring a body plan of reproducible proportions. Scaling has been observed in many biological systems [37, 68, 83, 122, 120], including the *Drosophila* wing imaginal disc [131]. The scale-invariance of the Dpp gradient was experimentally observed in mutants of the insulin pathway, which affects the wing disc size [112].

When cell division and proliferation depend on morphogen signaling, the morphogen gradient scales with the growing tissue size (Fig. 5). In mathematical descriptions, the growing tissue is represented by a moving boundary, and a perfect scaling of the morphogen gradient with the growing tissue size is defined as a scaling solution, i.e., a time-independent function $F(x)$ exists for all $x \in [0,1]$ such that

$$[\mathrm{L}](X,t) = [\mathrm{L}](0,t)F\left(\frac{X}{X_{\max}(t)}\right) \text{ for all } X \in [0, X_{\max}(t)], \tag{44}$$

where $X_{\max}(t)$ represents half size of the growing tissue.

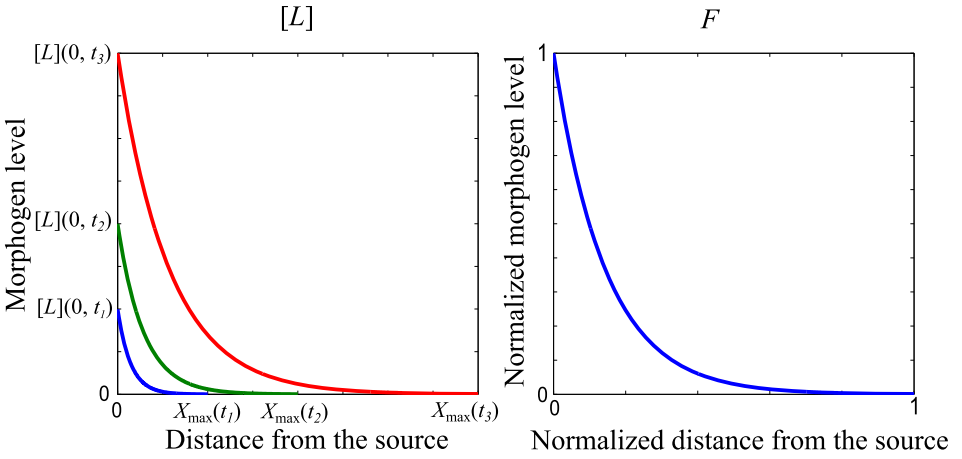

Figure 5: Illustration of perfect scale-invariance of morphogen gradient with growing tissue size. Left panel: blue line represents the morphogen at time t_1; green line represents the morphogen at time t_2; red line represents the morphogen at time t_3. We set $X_{\max}(t_2) = 2X_{\max}(t_1)$ and $X_{\max}(t_3) = 2X_{\max}(t_2)$. (Color figure online.)

For tissue growth control, recent experimental and theoretical studies supported that scale-invariance in the morphogen gradients may be a key factor for achieving robust patterning, spatially uniform growth, and a finite tissue size [6, 62, 131, 127]. In this section, we discuss some models for the scaling of morphogen gradients with tissue size.

In [91], a framework for studying the scale-invariance of a Turing system was proposed:

$$\frac{\partial[\mathrm{L}]}{\partial t} = \frac{\partial}{\partial X}(D_0 + D_1[\mathrm{E}]))\frac{\partial}{\partial X}[\mathrm{L}] + F([\mathrm{L}]), \tag{45}$$

$$\frac{\partial[\mathrm{E}]}{\partial t} = D_E\frac{\partial^2}{\partial X^2}[\mathrm{E}] + v_E. \tag{46}$$

Here, $X \in [-X_{\max}, X_{\max}]$ denotes the region of space occupied by the developing system. In this model, morphogen diffusion is affected by regulatory molecules so that the diffusion rate depends on [E], which denotes the concentration of regulatory molecules. The boundary conditions at $X = X_{\max}$ are:

$$\frac{\partial[\mathrm{L}]}{\partial X} = 0 \text{ and } -D_E\frac{\partial[\mathrm{E}]}{\partial X} = h[\mathrm{E}]. \tag{47}$$

The boundary conditions at $X = -X_{\max}$ are:

$$\frac{\partial[\mathrm{L}]}{\partial X} = 0 \text{ and } D_E \frac{\partial[\mathrm{E}]}{\partial X} = h[\mathrm{E}]. \tag{48}$$

Because the time scale of tissue growth is much longer than the time scale of morphogen dynamics, the study in [91] mainly focused on the steady state morphogen gradient. When the spatial coordinate is replaced by a dimensionless variable $\zeta = X/X_{\max} \in [-1, 1]$, the steady state system for morphogen concentration can be formulated as

$$\frac{1}{X_{\max}^2} \frac{\partial}{\partial \zeta} (D_0 + D_1[\hat{\mathrm{E}}]) \frac{\partial}{\partial \zeta} [\hat{\mathrm{L}}] + F([\hat{\mathrm{L}}]) = 0, \tag{49}$$

where $[\hat{\mathrm{L}}]$ and $[\hat{\mathrm{E}}]$ are the steady state concentrations of the morphogen and regulatory molecule, respectively. From equation (49), a simple and key condition for perfect scale invariance for the gradient [L] is that the morphogen diffusion coefficient $(D_0 + D_1[E])$ is proportional to the tissue size $X_{\max}^2$.

In [91], Turing stability analysis was applied to study the conditions for achieving perfect scale-invariance in a growing domain. The analysis showed that the coefficient of permeability for the leaky boundary condition, the parameter h, is the key to achieve scaling. With sufficiently large h, the range of $X_{\max}$ over which the growing pattern is essentially unchanged can be made as large as desired.

While [91] focused on the Turing system without sources at the boundary, the methods and model structure can be applied to the French flag type models discussed in this review. In [118], the author applied multiple time scale analysis to identify the conditions for the scale-invariance of the LED model. A model of the *Expansion-Repression* (ER) mechanism, was proposed for studying the scale-invariance of the morphogen system in the *Drosophila* wing disc [9, 10, 11].

The ER mechanism achieves scale-invariance in French flag model through the inhibition of morphogen degradation. Experiments have suggested that Dpp gradient formation, the diffusive molecule Pentagone (Pent) plays a role as an "expander" that is repressed by Dpp signaling and can expand the morphogen gradient by either enhancing morphogen diffusion or decreasing morphogen degradation [126]. If the expander inhibits morphogen degradation (Fig. 6), the dynamics of morphogen gradient formation can be modeled as

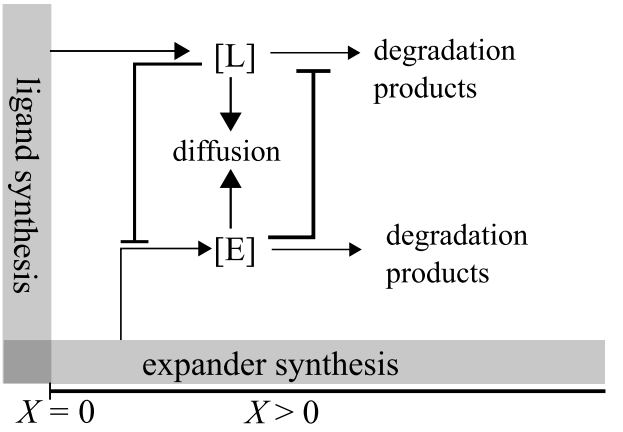

Figure 6: Illustration of the Expansion-Repression mechanism through regulation of morphogen degradation.

ER:

$$\frac{\partial[\mathrm{L}]}{\partial t} = D_L \frac{\partial^2[\mathrm{L}]}{\partial X^2} - \frac{\beta_L}{1+[\mathrm{E}]/E_0}[\mathrm{L}], \tag{50}$$

$$\frac{\partial[\mathrm{E}]}{\partial t} = D_E \frac{\partial^2[\mathrm{E}]}{\partial X^2} - \beta_E[\mathrm{E}] + \alpha_E \frac{T_{rep}^H}{T_{rep}^H + [\mathrm{L}]^H}, \tag{51}$$

where [E] denotes the concentration of the expander. The expander production is inhibited by the morphogen signaling and is represented by a Hill function. The morphogen is produced with a flux from $X = 0$ and reflective at the other boundary so that

$$\frac{\partial[\mathrm{L}]}{\partial X} = -j_{\mathrm{in}} \text{ and } \frac{\partial[\mathrm{E}]}{\partial X} = 0, \text{ at } X = 0; \tag{52}$$

$$\frac{\partial[\mathrm{L}]}{\partial X} = 0 \text{ and } \frac{\partial[\mathrm{E}]}{\partial X} = 0, \text{ at } X = X_{\max}. \tag{53}$$

As the expander accumulates, the degradation of the morphogen decreases, and the morphogen diffuses farther from the source, narrowing the region where the expander is expressed. With the assumption that the expander diffuses rapidly and degrades slowly, the distribution of the expander is approximately uniform across the field and continues to accumulate as long as it is produced. Under these conditions, the system reaches a steady state only when the expander production is repressed throughout the field [9, 10]. A scaling measurement was defined in these studies to discuss the conditions for achieving scale-invariance in morphogen systems.

In [75], the above model was modified by replacing the boundary condition (52) with a no flux boundary condition, and a narrow region of ligand production was introduced. Assuming that expanders rapidly diffuse and slowly degrade, the steady state system of the ER mechanism can be simplified to a one-equation boundary value problem for the steady state morphogen concentration $a(X)$:

$$D_L \frac{d^2 a}{dX^2} - \frac{\beta_L}{1 + b/E_0} a + V(X) = 0, \tag{54}$$

where

$$b = \frac{1}{\beta_E} \frac{\int_{-X_{\min}}^{X_{\max}} V_E(a(X)) dX}{X_{\max} + X_{\min}}, \tag{55}$$

and

$$V_E(y) = \alpha_E \frac{T_{rep}^H}{T_{rep}^H + y^H}. \tag{56}$$

Here, the function $V(X)$ is defined by the Heaviside function as (3). In this case, the existence and uniqueness of the steady state gradient were proven, and it was suggested that the ER mechanism could contribute to the robustness of morphogen-mediated patterning.

5.2. Moving boundary problem: from tissue growth to scaling of morphogen gradient

In the previous section, we discussed studies on the scaling of a steady state morphogen gradient. However, the motion field created by tissue growth may affect the dynamics of the morphogen gradient in the growing domain [22]. Tissue growth control and scaling of a morphogen gradient can be coupled through advection in a simple model. A generic model for a morphogen system on a growing domain was proposed by [35]. The model is based on the Reynolds transport theorem and is formulated as

$$\frac{\partial [\mathrm{L}]}{\partial t} + \frac{\partial (v[\mathrm{L}])}{\partial X} = D_L \frac{\partial^2 [\mathrm{L}]}{\partial X^2}, \quad \text{on } X \in (0, X_{\max}(t)), \tag{57}$$

where v denotes the growth field, and the domain is expanding linearly with time so that

$$X_{\max}(t) = X_{\max}(0) + v_g t. \tag{58}$$

The boundary condition is given by

$$\frac{\partial[\mathrm{L}]}{\partial X} = -j_{\mathrm{in}}, \quad \text{at } X = 0; \quad \frac{\partial[\mathrm{L}]}{\partial X} = 0, \quad \text{at } X = X_{\max}(t). \tag{59}$$

For a uniformly growing domain, the local growth rate $\partial v/\partial X$ is defined as

$$\frac{\partial v}{\partial X} = \frac{v_g}{X_{\max}(t)}. \tag{60}$$

In this system, morphogens spread, and an advection term is included because the morphogens may be attached to cells during tissue development. This inclusion is based on the fact that in the *Drosophila* wing disc, at least 97% of morphogens have been found either to be internalised or absorbed by cells [112, 140]. Because of the advection term, the dynamics is different from the previous models, in that the morphogen gradient does not reach a steady state within the physiological time scale.

Equation (57) can be rewritten in the following form:

$$\frac{\partial[\mathrm{L}]}{\partial t} + v\frac{\partial([\mathrm{L}])}{\partial X} = D_L\frac{\partial^2[\mathrm{L}]}{\partial X^2} - [\mathrm{L}]\frac{\partial v}{\partial X}. \tag{61}$$

In [35], the last term is called the dilution term, which is critical for perfect scaling in a uniformly growing domain. Simulations in [35] have showen that the morphogen gradient has perfect scaling when there is no diffusion ($D_L = 0$), which indicates that the impact of advective transport is essential for scale-invariance. This result was further verified in an *advective ligand extracellular diffusion model* (A-LED) involving reaction terms such as receptor binding and unbinding and morphogen internalization [35]:

A-LED:

$$\frac{\partial[\mathrm{L}]}{\partial t} + \frac{\partial(v[\mathrm{L}])}{\partial X} = D_L\frac{\partial^2[\mathrm{L}]}{\partial X^2} - k_{\mathrm{on}}[\mathrm{L}][\mathrm{R}_o] + k_{\mathrm{off}}[\mathrm{LR}_o] + V_{\mathrm{L}}(X,t) \tag{62}$$

$$\frac{\partial[\mathrm{R}_o]}{\partial t} + \frac{\partial(v[\mathrm{R}_o])}{\partial X} = -k_{\mathrm{on}}[\mathrm{L}][\mathrm{R}_o] + k_{\mathrm{off}}[\mathrm{LR}_o] - k_{\mathrm{in}}[\mathrm{R}_o] + k_{\mathrm{out}}[\mathrm{R}_i], \tag{63}$$

$$\frac{\partial[\mathrm{R}_i]}{\partial t} + \frac{\partial(v[\mathrm{R}_i])}{\partial X} = k_{\mathrm{in}}[\mathrm{R}_o] - k_{out}[\mathrm{R}_i] - k_{\mathrm{deg,R}}[\mathrm{R}_i] + V_{\mathrm{R}}(X,[\mathrm{LR}]), \tag{64}$$

$$\frac{\partial[\mathrm{LR}_o]}{\partial t} + \frac{\partial(v[\mathrm{LR}_o])}{\partial X} = k_{\mathrm{on}}[\mathrm{L}][\mathrm{R}_o] - k_{\mathrm{off}}[\mathrm{LR}_o] - k_{\mathrm{in}}[\mathrm{LR}_o] + k_{\mathrm{out}}[\mathrm{LR}_i], \tag{65}$$

$$\frac{\partial[\mathrm{LR}_o]}{\partial t}+\frac{\partial(v[\mathrm{LR}_o])}{\partial X}=k_{\mathrm{in}}[\mathrm{LR}_o]-k_{\mathrm{out}}[\mathrm{LR}_i] - k_{\mathrm{deg,LR}}[\mathrm{LR}_i], \tag{66}$$

$$[\mathrm{LR}]=[\mathrm{LR}_o]+[\mathrm{LR}_i], \tag{67}$$

where R_o, R_i, LR_o and LR_i denote the internal receptor, membrane-bound receptor, internal morphogen-receptor complex and membrane-bound morphogen-receptor complex, respectively.

5.3. Moving boundary problem: from morphogen gradient scaling to tissue growth

Experimental observations showed that cell division is strongly connected with the temporal dynamics of morphogen signaling [131]. In particular, the local growth rate is proportional to the relative temporal change of morphogen signaling. Based on this assumption and the Expansion-Repression mechanism, the *advection ER* (A-ER) system can be modeled by the following advection-reaction-diffusion equations [6]:

A-ER:

$$\frac{\partial[\mathrm{L}]}{\partial t}+\frac{\partial(v[\mathrm{L}])}{\partial X}=D_L\frac{\partial^2[\mathrm{L}]}{\partial X^2}-\frac{\beta_L}{1+[\mathrm{E}]/E_0}[\mathrm{L}], \tag{68}$$

$$\frac{\partial[\mathrm{E}]}{\partial t}+\frac{\partial(v[\mathrm{E}])}{\partial X}=D_E\frac{\partial^2[\mathrm{E}]}{\partial X^2}-\beta_E[\mathrm{E}]+\alpha_E\frac{T_{rep}^H}{T_{rep}^H+[\mathrm{L}]^H}. \tag{69}$$

The boundary condition is the same as (52)–(53) in the ER model, and the local growth rate $\partial v/\partial X$ is defined by the relative time derivative of the ligand concentration as

$$\frac{dv}{dX}=\frac{v_g}{[\mathrm{L}]}\frac{\partial[\mathrm{L}]}{\partial t}. \tag{70}$$

In the absence of expander, the ligand gradient satisfies

$$\frac{\partial[\mathrm{L}]}{\partial t}+\frac{\partial(v[\mathrm{L}])}{\partial X} = D_L\frac{\partial^2[\mathrm{L}]}{\partial X^2}-\beta_L[\mathrm{L}]. \tag{71}$$

An analytical study in [6] showed that scaling of the morphogen gradient implies a bounded tissue size at any time, resulting in a finite final tissue size at steady state. Furthermore, a finite final size leads to exponential decay morphogen gradients and uniform growth [6]. This result is consistent with experimental observations and provides a simple way to understand

how the final size of a tissue is regulated by the morphogen. In the presence of the expander, assuming that $D_E \gg 1$, further analysis showed that the system can also reach a finite tissue size, and the Expression-Repression feedback can increase the final tissue size and extend the time to reach the final size. Moreover, numerical studies suggested that Expression-Repression feedback can improve the robustness of the final tissue size to various model parameters.

Some investigators also consider tissue growth control through a spatial model, in which the local growth rate is assumed to be dependent on the slope or relative slope of the morphogen gradient [23, 100]. Based on the recent experimental data [100], it was proposed that the local growth rate might depend on the slope of the morphogen gradient and the concentration of the receptor [7]:

$$\frac{dv}{dX} = v_1 H\left(\left|\frac{\partial[\mathrm{L}]}{\partial X}\right| - c_L\right) + v_2 H([\mathrm{R}] - c_R), \tag{72}$$

where H is the Heaviside function. The numerical and analytic results showed that exponentially growth of the wing disc could be induced by uniform domain growth. However, this model does not include any mechanism for the termination of growth. Another approach of the spatial model is that the local growth rate depends on the relative spatial slope:

$$\frac{dv}{dX} = v_g \max\left(\frac{1}{[\mathrm{L}]}\left|\frac{\partial[\mathrm{L}]}{\partial X}\right| - c, 0\right), \tag{73}$$

where c is a constant to control the final size. If the relative slope $|\partial[\mathrm{L}]/\partial X|/[\mathrm{L}]$ is smaller than c, then the local growth rate becomes zero, and the tissue reaches its final size. The assumption of the relative slope model provides a potential answer for growth control; however, some experimental data challenge this hypothesis [103, 131]. Moreover, in this model, it is not clear how the cells robustly translate the noisy slope information to growth signaling when there is cell-to-cell variability.

5.4. Vertex models: mechanical feedback as a regulator of tissue growth

Mechanical feedback from stress and compression has also been hypothesized to modulate morphogen-mediated cell proliferation [1, 2, 106]. In [1], the size of the wing imaginal disc of *Drosophila* was investigated by considering the interplay between tissue growth and mechanical forces. In the study,

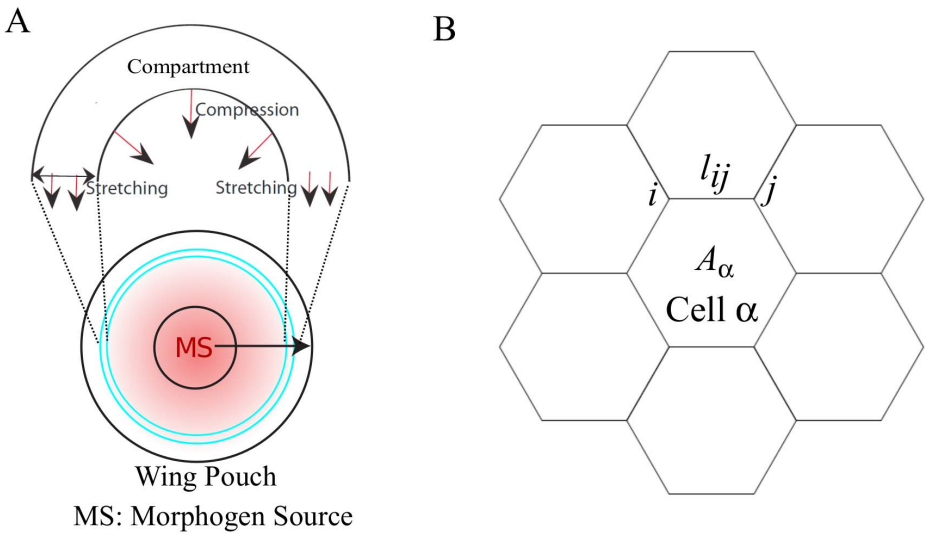

Figure 7: Illustrations of the mechanical feedback model. (A) Ring-shaped compartment-based model for wing imaginal disc of *Drosphila* in [1]. Distribution of Dpp is shown in red. (B) Vetex model of general tissue shape in [31]. (Color figure online.)

the wing pouch was approximately modeled as a radially symmetrical, two-dimensional elastic sheet with constant cell density, and the domain was discretized into several ring-shape compartments along the radius from the center (Fig. 7A). The model proposed that tissue growth is stimulated by high-level morphogen signaling at the center of the disc but is inhibited by increasing compression from the peripheral regions. Mechanical stretching in the peripheral regions induces growth even though morphogen levels are not above a particular threshold for inducing growth [1]. Based on these assumptions, uniform growth and finite final tissue size can be obtained from the model. However, the assumption of a radially symmetric wing pouch is not consistent with the actual wing pouch shape in experiments.

Several vertex models were proposed for the study of mechanical force balance in tissue developmental processes [2, 31, 33, 46]. Vertex models can be used to approximate the general shape of epithelial tissues by modeling cells with two-dimensional polygons (Fig. 7B). In [31] and [2], cell shapes are calculated by minimizing the energy

$$E = \sum_{\alpha} \frac{K_\alpha}{2}(A_\alpha - A_\alpha^{(0)})^2 + \sum_{<i,j>} \Lambda_{ij} l_{ij} + \sum_{\alpha} \frac{\Gamma_\alpha}{2} L_\alpha^2, \tag{74}$$

where $A^{(0)}$ denotes a target cell area, l_{ij} denotes the junction length between nodes i and j, and L denotes a cell perimeter. The energy function describes forces due to cell elasticity, actin-myosin bundles, and adhesion molecules [31]. This model provides a way to investigate the role of mechanical forces in cell topology. Using this vertex model, it was shown that growth control by mechanical forces can explain uniform growth, and the tissue can robustly reaches a finite size [2]. In [2], regulatory signaling pathways were included in the wing pouch model to explicitly connect mechanicals forces with growth control. This model further explains how mechanical feedbacks can regulate tissue growth at the molecular level. Numerical simulations showed that the model can account for growth termination as well as for the paradoxical observation that growth occurs uniformly in the presence of a non-uniform morphogen gradient and non-uniformly in the presence of a uniform morphogen gradient.

Mechanical feedback as a plausible mechanism of growth control is supported by many theoretical and experimental studies [19]. Nevertheless, currently, morphogen gradient formation has not been discussed in most studies of mechanical feedback regulation [1, 2, 46]. In these studies, the morphogen gradients in the models were usually explicitly formulated as an exponentially decreasing function from the source to the far boundary. Some models also involved scaling of the morphogen gradients [1, 2]. However, this approach cannot capture how the mechanical forces affect the morphogen gradient formation.

6. Conclusions and prospects

Remarkable progress has been made during the past 20 years in understanding morphogen-mediated patterning due to the rapid advance of experimental techniques and, most importantly, the involvement of mathematical modeling in recent years. The major contribution of mathematical models is in the areas of morphogen gradient formation and the mechanisms controlling the gradient. The models, many of which can now directly relate to experimental data, have been valuable in explaining how morphogen gradients form, how this information is translated into their target genes, how other diffusive molecules contribute to precise and robust morphogen-mediated signaling, how and why feedback regulations improve robustness and timing in morphogen dynamics, and how morphogen gradients regulate organ size. It has become increasingly clear that the interplay between experiments and mathematics is critical to establishing general theories that can make sense of the mechanistic complexity of organismal development driven by morphogens [34, 47, 59].

While modeling has significantly enhanced our understanding of morphogens, many important mathematical questions associated with the models remain to be addressed, and many biological questions remain unanswered. On the experimental side, numerous aspects of morphogen systems need more study, such as cell fate specification [60, 84, 99, 134], the complex dynamics of bone morphogen protein (BMP) gradients [13, 41, 93], the coordination of patterning and growth by morphogens [41, 97, 130], the dynamics of morphogen signaling [51], the design principles underlying the objectives of robust and precise pattern formation [59, 61], and the control of organ size [94].

On the modeling side, more advanced models need to include elements such as downstream signaling pathways that regulate gene expression [107], the growth Hippo signaling pathway [20, 21, 115], the temporal integration of morphogen signals for noise reduction [12, 60], cell-to-cell contacts that modulate growth [2], multiple morphogens for improving robustness [42, 83, 116], cooperative feedback loops [139], the role of tissue geometry in pattern formation [119], and noise in morphogen gradients [5, 43, 44, 138].

On the side of mathematical analysis and computational tools, several major challenges and unanswered questions remain. How do we determine the conditions for the existence, uniqueness, and stability of steady state gradients? The existence and uniqueness of the solutions of such boundary value problems are not always obvious, especially when the morphogen system is coupled with multiple nonlinear feedback loops. How does the signaling gradient depend on model structures and undetermined parameters? What is the best way to study the robustness of morphogen systems? While the classical asymptotic theory may be useful, the perturbations observed in morphogen systems tend to be much larger than the values of "small parameters" that are critically important in applying asymptotic analysis. Another mathematical challenge is the study of dynamic tissue boundaries, which is directly linked to the modeling of tissue growth control. How do we estimate final tissue size when a morphogen gradient is coupled with cell division (moving boundary)? Finally, efficient numerical schemes are needed for simulating tissue patterning and growth, and many challenges arise when solving temporal-spatial stochastic systems, higher dimensional morphogen systems, growing and moving boundary problems, and models of complex geometries [25, 49, 89, 119].

Studying physical systems, such as water waves, drops, and bubbles, has led to the establishment of the branch of mathematical and computational mechanics in mathematics and to the creation of many classical equations (e.g., Navier-Stokes equations) to which many mathematicians have devoted

their entire research. The modeling study of morphogen systems, a focus of this review, is introducing new equations and new methodologies for mathematics and computations [95]. Many characteristics, challenges, and questions associated with the complexity of morphogen systems will require new mathematics and new computational tools, likely leading to an emerging research area: mathematical and computational morphogenesis.

Acknowledgement

This work was partly supported by National Institutes of Health grants R01GM107264, R01ED023050, R01NS095355, P50GM76516, R01GM67247, R01MH105427, R56AR064532, and DMS1562176 to QN; National Science Foundation grant DMS1161621 to QN; and National Natural Science Foundation of China grants NSFC91430101 and NSFC 11272169 to JL. WCL was supported by a ECS grant from the Research Grants Council of Hong Kong (Project No. 9048043) and a CityU StUp Grant (Project No. 7200437).

References

[1] Aegerter-Wilmsen, T., Aegerter, C. M., Hafen, E. and Basler, K. (2007). Model for the regulation of size in the wing imaginal disc of Drosophila. *Mech Develop* **124** 318–326.

[2] Aegerter-Wilmsen, T., Heimlicher, M. B., Smith, a. C., de Reuille, P. B., Smith, R. S., Aegerter, C. M. and Basler, K. (2012). Integrating force-sensing and signaling pathways in a model for the regulation of wing imaginal disc size. *J Cell Science* **125** 3221–3231.

[3] Affolter, M. and Basler, K. (2007). The Decapentaplegic morphogen gradient: from pattern formation to growth regulation. *Nat Rev Genet* **8** 663–674.

[4] Akiyama, T., Kamimura, K., Firkus, C., Takeo, S., Shimmi, O. and Nakato, H. (2008). Dally regulates Dpp morphogen gradient formation by stabilizing Dpp on the cell surface. *Dev Biol* **313** 408–419.

[5] Arias, A. M. and Hayward, P. (2005). Filtering transcriptional noise during development: concepts and mechanisms. *Nat Rev Genet* **7** 34–44.

[6] Averbukh, I., Ben-Zvi, D., Mishra, S. and N., B. (2014). Scaling morphogen gradients during tissue growth by a cell division rule. *Development* **141** 2150–2156.

[7] Baker, R. E. and Maini, P. K. (2007). A mechanism for morphogen-controlled domain growth. *J Math Biol* **54** 597–622. MR2295744

[8] Belenkaya, T. Y., Han, C., Yan, D., Opola, R. J., Khodoun, M., Liu, H. and Lin, X. (2004). *Drosophila* Dpp morphogen movement is independent of dynamin-mediated endocytosis but regulated by the glypican members of heparan sulfate proteoglycans. *Cell* **119** 231–244.

[9] Ben-Zvi, D. and Barkai, N. (2010). Scaling of morphogen gradients by an expansion-repression integral feedback control. *Proc Natl Acad Sci USA* **107** 6924–6929.

[10] Ben-Zvi, D., Pyrowolakis, G., Barkai, N. and Shilo, B. Z. (2011). Expansion-repression mechanism for scaling the Dpp activation gradient in drosophila wing imaginal discs. *Curr Biol* **21** 1391–1396.

[11] Ben-Zvi, D., Shilo, B. Z. and Barkai, N. (2011). Scaling of morphogen gradients. *Curr Opin Genet Dev* **21** 704–710.

[12] Bergmann, S., Sandler, O., Sberro, H., Shnider, S., Schejter, E., Shilo, B.-Z. and Barkai, N. (2007). Pre-steady-state decoding of the Bicoid morphogen gradient. *PLoS Biol* **5** e46.

[13] Bier, E. and De Robertis, E. M. (2015). BMP gradients: A paradigm for morphogen-mediated developmental patterning. *Science* **348** aaa5838.

[14] Bollenbach, T., Krus, K., Pantazis, P., González-Gaitán, M. and Jülicher, F. (2007). Morphogen transport in epithelia. *Phys Rev E* **75** 011901.

[15] Bollenbach, T., Kruse, K., Pantazis, P., González-Gaitán, M. and Jülicher, F. (2005). Robust formation of morphogen gradients. *Phys Rev Lett* **94** 1–4.

[16] Bollenbach, T., Pantazis, P., Kicheva, A., Bokel, C., Gonzalez-Gaitan, M. and Julicher, F. (2008). Precision of the Dpp gradient. *Development* **135** 1137–1146.

[17] Briscoe, J., P, L. and J, V., eds. (2010). *Generation and Interpretation of Morphogen Gradients*. Cold Spring Harbor, New York: Cold Spring Harb Lab.

[18] Briscoe, J. and Small, S. (2015). Morphogen rules: design principles of gradient-mediated embryo patterning. *Development* **142** 3996–4009.

[19] Buchmann, A., Alber, M. and Zartman, J. J. (2014). Sizing it up: The mechanical feedback hypothesis of organ growth regulation. *Semin Cell Dev Biol* **35** 73–81.

[20] Buttitta, L. a. and Edgar, B. a. (2007). How size is controlled: from Hippos to Yorkies. *Nat Cell Biol* **9** 1225–1227.

[21] Cho, E. and Irvine, K. D. (2004). Action of fat, four-jointed, dachsous and dachs in distal-to-proximal wing signaling. *Development* **131** 4489–4500.

[22] Crampin, E. J., Gaffney, E. a. and Maini, P. K. (1999). Reaction and diffusion on growing domains: scenarios for robust pattern formation. *Bull Math Biol* **61** 1093–1120.

[23] Day, S. J. and Lawrence, P. a. (2000). Measuring dimensions: the regulation of size and shape. *Development* **127** 2977–2987.

[24] Dessaud, E., Ribes, V., Balaskas, N., Yang, L. L., Pierani, A., Kicheva, A., Novitch, B. G., Briscoe, J. and Sasai, N. (2010). Dynamic assignment and maintenance of positional identity in the ventral neural tube by the morphogen sonic Hedgehog. *PLoS Biol* **8** e1000382.

[25] Du, X., Osterfield, M. and Shvartsman, S. Y. (2014). Computational analysis of three-dimensional epithelial morphogenesis using vertex models. *Phys Biol* **11** 066007.

[26] Eldar, A., Dorfman, R., Weiss, D., Ashe, H., Shilo, B.-Z. and Barkai, N. (2002). Robustness of the BMP morphogen gradient in Drosophila embryonic patterning. *Nature* **419** 304–308.

[27] Eldar, A., Dorfman, R., Weiss, D., Ashe, H., Shilo, B. Z. and Barkai, N. (2002). Robustness of the BMP morphogen gradient in Drosophila embryonic patterning. *Nature* **419** 304–308.

[28] Eldar, A., Rosin, D., Shilo, B. Z. and Barkai, N. (2003). Self-enhanced ligand degradation underlies robustness of morphogen gradients. *Dev Cell* **5** 635–646.

[29] Emberly, E. (2008). Optimizing the readout of morphogen gradients. *Phys Rev E* **77** 041903.

[30] Entchev, E. V., Schwabedissen, A. and Gonzalez-Gaitan, M. (2000). Gradient formation of the TGF-β homolog Dpp. *Cell* **103** 981–991.

[31] Farhadifar, R., Röper, J.-C., Aigouy, B., Eaton, S. and Jülicher, F. (2007). The influence of cell mechanics, cell-cell interactions, and proliferation on epithelial packing. *Curr Biol* **17** 2095–2104.

[32] Félix, M.-A. and Barkoulas, M. (2015). Pervasive robustness in biological systems. *Nat Rev Genet* **16** 483–496.

[33] Fletcher, A. G., Osterfield, M., Baker, R. E. and Shvartsman, S. Y. (2014). Vertex models of epithelial morphogenesis. *Biophys J* **106** 2291–2304.

[34] Freeman, M. (2002). Morphogen gradients, in theory. *Dev Cell* **2** 680–690.

[35] Fried, P. and Iber, D. (2014). Dynamic scaling of morphogen gradients on growing domains. *Nature Commun* **5** 5077.

[36] Gordon, P. V., Sample, C., Berezhkovskii, A. M., Muratov, C. B. and Shvartsman, S. Y. (2011). Local kinetics of morphogen gradients. *Proc Natl Acad Sci USA* **108** 6157–6162.

[37] Gregor, T., Bialek, W., de Ruyter van Steveninck, R. R., Tank, D. W. and Wieschaus, E. F. (2005). Diffusion and scaling during early embryonic pattern formation. *Proc Natl Acad Sci USA* **102** 18403–18407.

[38] Gregor, T., Tank, D. W., Wieschaus, E. F. and Bialek, W. (2007). Probing the limits to positional information. *Cell* **130** 153–164.

[39] Gurdon, J. B. and Bourillot, P. Y. (2001). Morphgen gradient interpretation. *Nature* **413** 797–803.

[40] Häcker, U., Nybakken, K. and Perrimon, N. (2005). Heparan sulphate proteoglycans: The sweet side of development. *Nat Rev Mol Cell Biol* **6** 530–541.

[41] Hamaratoglu, F., Affolter, M. and Pyrowolakis, G. (2014). Dpp/BMP signaling in flies: From molecules to biology. *Semin Cell Dev Biol* **32** 128–136.

[42] Hardway, H., Mukhopadhyay, B., Burke, T., Hichman, T. J. and Forman, R. (2008). Modeling the precision and robustness of hunchback border during drosophila embryonic development. *J Theor Biol* **254** 390–399.

[43] He, F., Ren, J., Wang, W. and Ma, J. (2012). Evaluating the *Drosophila* Bicoid morphogen gradient system through dissecting the noise in transcriptional bursts. *Bioinformatics* **28** 970–975.

[44] Holloway, D. M., Lopes, F. J. P., da Fontoura Costa, L., Travençolo, B. A. N., Golyandina, N., Usevich, K. and Spirov, A. V. (2011). Gene expression noise in spatial patterning: *hunchback* promoter structure affects noise amplitude and distribution in *Drosophila* segmentation. *PLoS Comput Biol* **7** e1001069. MR2788141

[45] Houchmandzadeh, B., Wieschaus, E. and Leibler, S. (2002). Establishment of developmental precision and proportions in the early Drosophila embryo. *Nature* **415** 798–802.

[46] Hufnagel, L., Teleman, A. a., Rouault, H., Cohen, S. M. and Shraiman, B. I. (2007). On the mechanism of wing size determination in fly development. *Proc Natl Acad Sci USA* **104** 3835–3840.

[47] Ibañes, M. and Belmonte, J. C. I. (2008). Theoretical and experimental approaches to understand morphogen gradients. *Mol Syst Biol* **4** 176.

[48] Kam, R. K. T., Deng, Y., Chen, Y. and Zhao, H. (2012). Retinoic acid synthesis and functions in early embryonic development. *Cell & Bioscience* **2** 11.

[49] Kang, H.-W., Zheng, L. and Othmer, H. G. (2012). A new method for choosing the computational cell in stochastic reaction–diffusion systems. *J Math Biol* **65** 1017–1099. MR2993939

[50] Kerszberg, M. and Wolpert, L. (1998). Mechanisms for positional signalling by morphogen transpot: a theoretical study. *J Theor Biol* **191** 103–114.

[51] Kicheva, A. and Briscoe, J. (2015). Developmental Pattern Formation in Phases. *Trend Cell Biol* **25** 579–591.

[52] Kicheva, A., Pantazis, P., Bollenbach, T., Kalaidzidis, Y., Bittig, T., Jülicher, F. and Gonaález-Gaitán, M. (2007). Kinetics of morphogen gradient formation. *Science* **315** 521–525.

[53] Kirkpatrick, C. A., Dimitroff, B. D., Rawson, J. M. and Selleck, S. B. (2004). Spatial regulation of Wingless morphgen dirstribution and signaling by Dally-like protein. *Dev Cell* **7** 513–523.

[54] Kirkpatrick, C. A. and Selleck, S. B. (2007). Heparan sulfate proteoglycans at a glance. *J Cell Science* **120** 1829–1832.

[55] Kondo, S. and Miura, T. (2010). Reaction-diffusion model as a framework for understanding biological pattern formation. *Science* **329** 1616–1620. MR2732467

[56] Kushner, T., Simonyan, A. and Wan, F. Y. M. (2014). A new approach to feedback for robust signaling gradients. *Studies in Appl Math* **133** 18–51. MR3244957

[57] Lander, A., Nie, Q. and Wan, F. Y. M. (2002). Do morphogen gradients arise by diffusion? *Dev Cell* **2** 785–796.

[58] Lander, A. D. (2007). Morpheus unbound: reimagining the morphogen gradient. *Cell* **128** 245–256.

[59] Lander, A. D. (2011). Pattern, growth, and control. *Cell* **144** 955–969.

[60] Lander, A. D. (2013). How cells know where they are. *Science* **339** 923–927.

[61] Lander, A. D., Lo, W. C., Nie, Q. and Wan, F. Y. M. (2009). The measure of success: constraints, objectives, and tradeoffs in morphogen-mediated patterning. *Cold Spring Harb Perspect Biol* **1** a002022.

[62] Lander, A. D., Nie, Q., Vargas, B. and Wan, F. Y. M. (2011). Size-normalized robustness of dpp gradient in *Drosophila* wing imaginal disc. *J Mech Mater Struct* **6** 321–350.

[63] Lander, A. D., Nie, Q. and Wan, F. Y. M. (2005). Spatially distributed morphogen production and morphogen gradient formation. *Math Biosci Eng* **2** 239–262. MR2144238

[64] Lander, A. D., Nie, Q. and Wan, F. Y. M. (2005). Aggregation of a distribution source in morphogen gradient formation. *Studies in Appl Math* **114** 343–374. MR2131551

[65] Lander, A. D., Nie, Q. and Wan, F. Y. M. (2005). Multiple paths to morphogen gradient robustness. preprint.

[66] Lander, A. D., Nie, Q. and Wan, F. Y. M. (2007). Membrane-associated non-receptors and morphogen gradients. *Bull Math Biol* **69** 33–54. MR2320697

[67] Lander, A. D., Nie, Q., Wan, F. Y. M. and Zhang, Y. T. (2009). Localized ectopic expression of Dpp receptors in a Drosophila embryo. *Studies in Appl Math* **123** 174–214. MR2547947

[68] Lauschke, V. M., Tsiairis, C. D., Francois, P. and Aulehla, A. (2013). Scaling of embryonic patterning based on phase-gradient encoding. *Nature* **493** 101–105.

[69] Lawrence, P. A. and Morata, G. (1977). The early development of mesothoracic compartments in Drosophila. An analysis of cell lineage and fate mapping and an assessment of methods. *Dev Biol* **56** 40–51.

[70] Lei, J. Z. (2010). Mathematical model of the Dpp gradient formation in drosophila wing imagincal disc. *Chinese Sci Bull* **55** 984–991.

[71] Lei, J. and Song, Y. (2010). Mathematical model of the formation of morphogen gradients through membrane-associated non-receptors. *Bull Math Biol* **72** 805–829. MR2609390

[72] Lei, J., Wan, F. Y. M., Lander, A. and Nie, Q. (2011). Robustness of signaling gradient in drosophila wing imaginal disc. *Discrete Contin Dyn Syst B* **16** 835–866. MR2806325

[73] Lei, J., Wang, D., Song, Y., Nie, Q. and Wan, F. Y. M. (2012). Robustness of Morphogen gradients with "bucket brigade" transport through membrane-associated non-receptors. *Discrete Contin Dyn Syst B* **18** 721–739. MR3007751

[74] Lin, X. (2004). Functions of heparan sulfate proteoglycans in cell signaling during development. *Development* **131** 6009–6021.

[75] Lo, W. C. (2014). Morphogen gradient with expansion-repression mechanism: Steady-state and robustness studies. *Discrete Contin Dyn Syst B* **19** 775–787. MR3180727

[76] Lo, W.-C., Zhou, S., Wan, F. Y. M., Lander, A. D. and Nie, Q. (2015). Robust and precise morphogen-mediated pattering: trade-offs, constraints and mechanisms. *J R Soc Interface* **12** 20141041.

[77] Lopes, F. J. P., Vieira, F. M. C., Holloway, D. M., Bisch, P. M. and Spirov, A. V. (2008). Spatial bistability generates *hunchback* expression sharpness in the *Drosophila* embryo. *PLoS Comput Biol* **4** e1000184. MR2448489

[78] Lou, Y., Nie, Q. and Wan, F. Y. M. (2005). Effects of Sog on Dpp-receptor binding. *SIAM J Appl Math* **65** 1748–1771. MR2177723

[79] Lou, Y., Nie, Q. and Wan, F. Y. M. (2004). Nonlinear eigenvalue problems in the stability analysis of morphogen gradients. *Studies in Appl Math* **113** 183–215. MR2069857

[80] Maini, P. K., Woolley, T. E., Baker, R. E., Gaffney, E. A. and Lee, S. S. (2012). Turing's model for biological pattern formation and the robustness problem. *Interface Focus* **2** 487–496.

[81] Martin, F. A. and Morata, G. (2006). Compartments and the control of growth in the Drosophila wing imaginal disc. *Development* **133** 4421–4426.

[82] Matsuo, I. and Kimura-Yoshida, C. (2014). Extracellular distribution of diffusible growth factors controlled by heparan sulfate proteoglycans during mammalian embryogenesis. *Philos Trans R Soc London B: Biol Sci* **369** 20130545.

[83] McHale, P., Rappel, W.-J. and Levine, H. (2006). Embryonic pattern scaling achieved by oppositely directed morphogen gradients. *Phys Biol* **3** 107–120.

[84] Meinhardt, H. (2009). Models for the generation and interpretation of gradients. *Cold Spring Harb Perspect Biol* **1** a001362.

[85] Mizutani, C. M., Nie, Q., Wan, F. Y. M., Zhang, Y.-T., Vilmos, P., Sousa-Neves, R., Bier, E., Marsh, J. L. and Lander, A. D. (2005). Formation of the BMP activity gradient in the Drosophila embryo. *Dev Cell* **8** 915–924.

[86] Morelli, L. G., Uriu, K., Ares, S. and Oates, A. C. (2012). Computational approaches to developmental pattering. *Science* **336** 187–191. MR2954190

[87] Morimura, S., Maves, L., Chen, Y. and Hoffmann, F. M. (1996). decapentaplegic overexpression affects Drosophila wing and leg imaginal disc development and wingless expression. *Dev Biol* **177** 136–151.

[88] Morishita, Y. and Iwasa, Y. (2008). Optimal placement of multiple morphogen sources. *Phys Rev E* **77** 041909.

[89] Murisic, N., Hakim, V., Kevrekidis, I. G., Shvartsman, S. Y. and Audoly, B. (2015). From discrete to continuum models of three-dimensional deformations in epithelial sheets. *Biophy J* **109** 154–163.

[90] Nellen, D., Burke, R., Struhl, G. and Basler, K. (1996). Direct and long-range action of a DPP morphogen gradient. *Cell* **85** 357–368.

[91] Othmer, H. G. and Pate, E. (1980). Scale-invariance in reaction-diffusion models of spatial pattern formation. *Proc Natl Acad Sci USA* **77** 4180–4184.

[92] Pfeiffer, S. and Vincent, J.-P. (1999). Signalling at a distance: transport of wingless in the embryonic epidermis of Drosophila. *Semin Cell Dev Biol* **10** 303–309.

[93] Plouhinec, J. L., Zakin, L. and De Robertis, E. M. (2011). Systems control of BMP morphogen flow in vertebrate embryos. *Curr Opin Genet Dev* **21** 696–703.

[94] Powell, A. E. and Lenhard, M. (2012). Control of organ size in plants. *Curr Biol* **22** R360–R367.

[95] Reed, M. C. (2015). Mathematical biology is good for mathematics. *Notices of the AMS* **62** 1172–1176.

[96] Reeves, G. T. and Fraser, S. E. (2009). Biological systems from an engineer's point of view. *PLoS Biol* **7** e1000021.

[97] Restrepo, S., Zartman, J. J. and Basler, K. (2014). Coordination of patterning and growth by the morphogen DPP. *Curr Biol* **24** R245–R255.

[98] Richards, D. M. and Saunders, T. E. (2015). Spatiotemporal analysis of different mechanisms for interpreting morphogen gradients. *Biophys J* **108** 2061–2073.

[99] Rogers, K. W. and Schier, A. F. (2011). Morphogen Gradients: From Generation to Interpretation. *Annu Rev Cell Dev Biol* **27** 377–407.

[100] Rogulja, D. and Irvine, K. D. (2005). Regulation of cell proliferation by a morphogen gradient. *Cell* **123** 449–461.

[101] Schwank, G. and Basler, K. (2010). Regulation of organ growth by morphogen gradients. *Cold Spring Harb Perspect Biol* **2** a001669.

[102] Schwank, G., Dalessi, S., Yang, S.-F., Yagi, R., de Lachapelle, A. M., Affolter, M., Bergmann, S. and Basler, K. (2011). Formation of the long range Dpp morphogen gradient. *PLoS Biol* **9** e1001111.

[103] Schwank, G., Restrepo, S. and Basler, K. (2008). Growth regulation by Dpp: an essential role for Brinker and a non-essential role for graded signaling levels. *Development* **135** 4003–4013.

[104] Shilo, B.-Z., Haskel-Ittah, M., Ben-Zvi, D., Schejter, E. D. and Barkai, N. (2013). Creating gradients by morphogen shuttling. *Trend Genet* **29** 339–347.

[105] Shimmi, O., Umulis, D., Othmer, H. and O'Connor, M. (2005). Facilitated transport of a Dpp/Scw heterodimer by Sog/Tsg patterns the dorsal surface of the Drosophila blastoderm embryo. *Cell* **120** 873–886.

[106] Shraiman, B. I. (2005). Mechanical feedback as a possible regulator of tissue growth. *Proc Natl Acad Sci USA* **102** 3318-3323.

[107] Shvartsman, S. Y. and Baker, R. E. (2012). Mathematical models of morphogen gradients and their effects on gene expression. *Dev Biol* **1** 715–730.

[108] Simonyan, A. and Wan, F. Y. M. (2016). Transient feedback and robust signaling gradients. *Int J Num Anal Mod* **13** 179–204. MR3421773

[109] Smith, J. C. (2009). Forming and interpreting gradients in the early Xenopus embryo. *Cold Spring Harb Perspect Biol* **1** a002477.

[110] Smith, J. C., Hagemann, A., Saka, Y. and Williams, P. H. (2008). Understanding how morphogens work. *Philos Trans R Soc London B: Biol Sci* **363** 1387–1392.

[111] Tabata, T. (2001). Genetics of morphogen gradients. *Nat Rev Genet* **2** 620–630.

[112] Teleman, A. A. and Cohen, S. M. (2000). Dpp gradient formation in the Drosophila wing imaginal disc. *Cell* **103** 971–980.

[113] The, I., Bellaiche, Y. and Perrimon, N. (1999). Hedgehog movement is regulated through *tout velu*-dependent synthesis of a heparan sulfate proteoglycan. *Mol Cell* **4** 633–639.

[114] Theisen, H., Syed, A., Nguyen, B. T., Lukacsovich, T., Purcell, J., Srivastava, G. P., Iron, D., Gaudenz, K., Nie, Q., Wan, F. Y. M., Waterman, M. L. and Marsh, J. L. (2007). Wingless directly represses DPP morphogen expression via an Armadillo/TCF/Brinker complex. *PLoS ONE* **2** e142.

[115] Thompson, B. J. and Cohen, S. M. (2006). The Hippo pathway regulates the bantam microRNA to control cell proliferation and apoptosis in Drosophila. *Cell* **126** 767–774.

[116] Tostevin, F., ten Wold, P. R. and Howard, M. (2007). Fundamental limits to position determination by concentration gradients. *PLoS Comput Biol* **3** e78. MR2373053

[117] Umulis, D., O'Connor, M. B. and Othmer, H. G. (2008). Robustness of embryonic spatial patterning in Drosophila melanogaster. *Curr Top Dev Biol* **81** 65–111.

[118] Umulis, D. M. (2009). Analysis of dynamic morphogen scale invariance. *J R Soc Interface* **6** 1179–1191.

[119] Umulis, D. M. and Othmer, H. G. (2012). The importance of geometry in mathematical models of developing systems. *Curr Opin Genet Dev* **22** 547–552.

[120] Umulis, D. M. and Othmer, H. G. (2013). Mechanisms of scaling in pattern formation. *Development* **140** 4830–4843.

[121] Umulis, D. M. and Othmer, H. G. (2014). The Role of Mathematical Models in Understanding Pattern Formation in Developmental Biology. *Bull Math Biol* **77** 817–845. MR3350424

[122] Umulis, D. M., Shimmi, O., O'Connor, M. B. and Othmer, H. G. (2010). Organism-scale modeling of early Drosophila patterning via bone morphogenetic proteins. *Dev Cell* **18** 260–274.

[123] Vergas, B. (2006). Leaky boundaries and morphogen gradietns PhD thesis, Dept. of Math., University of California, Irvine.

[124] von Dassow, G., Meir, E., Munro, E. M. and Odell, G. M. (2000). The segment polarity network is a robust developmental module. *Nature* **406** 188–192.

[125] von Dassow, G. and Odell, G. M. (2002). Design and constraints of the Drosophila segment polarity module: robust spatial patterning emerges from intertwined cell state switches. *J Exp Zool* **294** 179–215.

[126] Vuilleumier, R., Springhorn, A., Patterson, L., Koidl, S., Hammerschmidt, M., Affolter, M. and Pyrowolakis, G. (2010). Control of Dpp morphogen signalling by a secreted feedback regulator. *Nat Cell Biol* **12** 611–617.

[127] Wartlick, O., Jülicher, F. and Gonzalez-Gaitan, M. (2014). Growth control by a moving morphogen gradient during Drosophila eye development. *Development* **141** 1884–1893.

[128] Wartlick, O., Kicheva, A. and Gonaález-Gaitán, M. (2009). Morphogen gradient formation. *Cold Spring Harb Perspect Biol* **1** a001255.

[129] Wartlick, O., Mumcu, P., Jülicher, F. and Gonaález-Gaitán, M. (2012). Response to comment on "Dynamics of Dpp signaling and proliferation control". *Science* **335** 401.

[130] Wartlick, O., Mumcu, P., Jülicher, F. and Gonzalez-Gaitan, M. (2011). Understanding morphogenetic growth control - lessons from flies. *Nat Rev Mol Cell Biol* **12** 594–604.

[131] Wartlick, O., Mumcu, P., Kicheva, a., Bittig, T., Seum, C., Jülicher, F. and González-Gaitán, M. (2011). Dynamics of Dpp signaling and proliferation control. *Science* **331** 1154–1159.

[132] White, R., Nie, Q., Lander, A. D. and Schilling, T. (2007). Complex Regulation of cyp26a1 Creates a Robust Retinoic Acid Gradient in the Zebrafish Embryo. *PLoS Biol* **5** e304.

[133] Wolpert, L. (1969). Positional Information and Spatial Pattern of Cellular Differentiation. *J Theor Biol* **25** 1–47.

[134] Wolpert, L. (2011). Positional information and patterning revisited. *J Theor Biol* **269** 359–365.

[135] Wolpert, L. and Tickle, C. (2010). *Principles of Development*. Oxford, Academic Press.

[136] Woolley, T. E., Baker, R. E., Gaffney, E. a. and Maini, P. K. (2011). Stochastic reaction and diffusion on growing domains: Understanding the breakdown of robust pattern formation. *Phys Rev E* **84** 1–16.

[137] Yan, D. and Lin, X. (2009). Shaping morphogen gradients by proteoglycans. *Cold Spring Harb Perspect Biol* **1** a002493.

[138] Zhang, L., Radtke, K., Zheng, L., Cai, A. Q., Schilling, T. F. and Nie, Q. (2012). Noise drives sharpening of gene expression boundaries in the zebrafish hindbrain. *Mol Syst Biol* **8** 613.

[139] Zhang, Y.-T., Lander, A. D. and Nie, Q. (2007). Computational analysis of BMP gradients in dorsal-ventral pattering of the zebrafish emnbryo. *J Theor Biol* **248** 579–589. MR2899082

[140] Zhou, S., Lo, W. C., Suhalim, J. L., Digman, M. A., Gratton, E., Nie, Q. and Lander, A. D. (2012). Free extracellular diffusion creates the Dpp morphogen gradient of the Drosophila wing disc. *Curr Biol* **22** 668–675.

Jinzhi Lei
Zhou Pei-Yuan Center for Applied Mathematics
MOE Key Laboratory of Bioinformatics
Tsinghua University
Beijing 100084
China
E-mail address: jzlei@tsinghua.edu.cn

Wing-Cheong Lo
Department of Mathematics
City University of Hong Kong
Kowloon
Hong Kong
E-mail address: wingclo@cityu.edu.hk

Qing Nie
Department of Mathematics
Department of Biomedical Engineering
Center for Complex Biological Systems
Center for Mathematical and Computational Biology
University of California, Irvine
Irvine, CA 92697-3875
USA
E-mail address: qnie@math.uci.edu

Received December 5, 2015